Article

Human gut M cells resemble dendritic cells and present gluten antigen

https://doi.org/10.1038/s41586-025-09829-8

Received: 3 September 2024

Accepted: 29 October 2025

Published online: 10 December 2025

Open access

Check for updates

Daisong Wang[1,2,13], Sangho Lim[1,2,13], Willine J. van de Wetering[3], Carmen Lopez-Iglesias[3], Yuu Okura[4], Yuri Teranishi-Ikawa[4], Akihiko Mizoroki[4], Willem Kasper Spoelstra[5], Talya Dayton[1,2,12], Gijs J. F. van Son[6], Apollo Pronk[7], Niels Smakman[7], Gieneke B. C. Gonera-de Jong[8], Sebo Withoff[9], Iris H. Jonkers[9], Jeroen S. van Zon[5], Sander J. Tans[5,10], Peter J. Peters[3], Johan H. van Es[1,2] & Hans Clevers[1,2,6,11] ✉

Microfold (M) cells are rare intestinal epithelial cells that reside in the follicle-associated epithelium of Peyer's patches[1]. M cells transport luminal antigens to submucosal antigen-presenting cells[2,3]. These insights primarily derive from transmission electron microscopy and studies using genetically modified mice[2–4]. Here we establish an intestinal organoid model to study human M cells and reconstruct the differentiation trajectory of M cells through transcriptome profiling. The results indicate that as well as facilitating luminal antigen transport, human M cells also directly present antigens via the class II major histocompatibility complex (MHC-II). Notably, the related enterocytes only express MHC-II in chronic inflammatory states and do not express typical dendritic cell markers. Human M cells physiologically express a gene profile that resembles that of dendritic cells. Similar to dendritic cells, M cell development is induced by RANKL and CSF2 and requires the transcription factors SPIB and RUNX2. HLA-DQ2.5 M cells process and present gluten antigen as demonstrated in organoid–T cell co-culture assays. These findings suggest that M cells may have a central role in coeliac disease.

M cells are rare epithelial cells that are involved in intestinal mucosal immunity[1–3]. They have irregular microvilli on their apical surface[4,5] and transcytose luminal antigens to the immune cells that reside in their basally located 'pocket'[2–4]. Mouse M cells are derived from LGR5$^+$ intestinal stem cells[6], require RANKL[7] and the transcription factors SPIB[6,8] and SOX8 (ref. 9), and express *Gp2* (ref. 10). The differentiation trajectory of human M cells has largely remained unknown. Mouse M cell markers are often not expressed in humans—for example, *Ulex europaeus* agglutinin-1 (UEA-1) uniquely recognizes mouse M cells[11], whereas human M cells display sialyl Lewis A antigen[12]. Of note, the M cell pocket contains both dendritic cells and T cells[13]. M cells may directly interact with T cells through a dendritic cell-independent mechanism.

Human M cell organoids

We recently developed a culture protocol for human intestinal organoids[14], which we further optimized as 'M cell medium' by adding RANKL, tumour necrosis factor (TNF) and retinoic acid, leading to the appearance of GP2$^+$ cells (Fig. 1a–c). Consistent with observations in mice[7], RANKL appeared to be essential for the development of M cell organoids (Fig. 1b,c). M cell organoids exhibited reduced numbers of proliferative buds (Extended Data Fig. 1a–d), as noted previously for mouse M cell organoids[15]. As previously reported[16], lymphotoxin-β (LTB) enhanced the frequency of GP2$^+$ cells but led to cell death in our culture (Extended Data Fig. 1e,f). LTB had little effect on absolute numbers of M cells and was thus excluded from the differentiation cocktail.

We next created *SPIB* reporter organoids (SPIB-P2A-tdTomato; Extended Data Fig. 1g). M cell medium efficiently generated *SPIB*-expressing (tdTomato$^+$) cells (Extended Data Fig. 1h). Immunofluorescent staining and flow cytometry analysis revealed that *SPIB* expression was induced in more than 75% of cells, with approximately 3% co-expressing GP2 on their apical surface (Fig. 1d,e). These SPIB$^+$GP2$^+$ cells expressed other M cell markers such as *SOX8* and *CCL23* (ref. 16), as demonstrated by quantitative PCR (qPCR) analysis following fluorescence-activated cell sorting (FACS) (Extended Data Fig. 1i). Cells derived from M cell organoids were sorted by FACS for single-cell RNA-sequencing (scRNA-seq) analysis. We thereby identified three cell clusters corresponding to enterocytes, intermediate cells and M cells (Fig. 1f,g and Extended Data Fig. 1j,k).

To identify marker genes for primary M cells, we re-analysed the published scRNA-seq resource[17], which reportedly contained around 400 M cells among more than 420,000 total cells. This dataset was integrated with three other scRNA-seq datasets that covered all other intestinal cell types (Extended Data Fig. 1l). We noted that more than half of the previously annotated M cells expressed *GP2* but no other M cell markers (Extended Data Fig. 1l,m). These cells were marked by *TFF2* and *PGC* and derived from the duodenum (Extended Data Fig. 1m,n). GP2 is known to mark human Brunner's gland cells[18]. Immunohistochemistry

[1]Hubrecht Institute, Royal Netherlands Academy of Arts and Sciences, UMC Utrecht, Utrecht, The Netherlands. [2]Oncode Institute, Utrecht, The Netherlands. [3]The Microscopy CORE Lab, Maastricht University, Maastricht, The Netherlands. [4]Chugai Pharmaceutical, Tokyo, Japan. [5]AMOLF Institute, Amsterdam, The Netherlands. [6]The Princess Máxima Center for Pediatric Oncology, Utrecht, The Netherlands. [7]Department of Surgery, Diakonessenhuis Utrecht and Zeist, Utrecht, The Netherlands. [8]Department of Pediatrics, Wilhelmina Hospital Assen, Assen, The Netherlands. [9]Department of Genetics, University of Groningen, University Medical Center Groningen, Groningen, The Netherlands. [10]Department of Bionanoscience, Kavli Institute of Nanoscience Delft, Delft University of Technology, Delft, The Netherlands. [11]Institute of Human Biology (IHB), Roche Pharma Research and Early Development, Roche Innovation Center, Basel, Switzerland. [12]Present address: Tissue Biology and Disease Modeling Unit, EMBL, Barcelona, Spain. [13]These authors contributed equally: Daisong Wang, Sangho Lim. ✉e-mail: h.clevers@hubrecht.eu

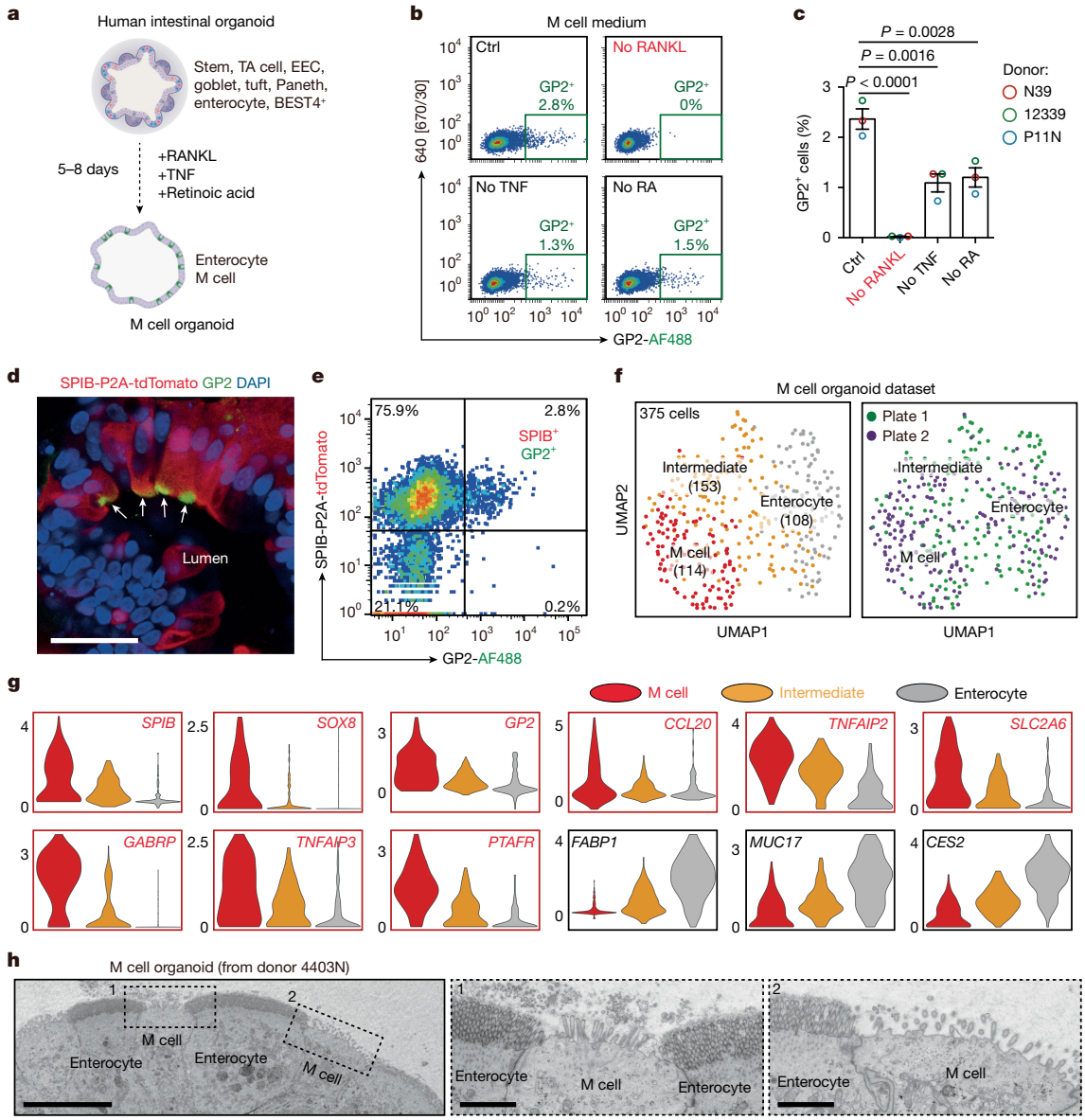

Fig. 1 | A human intestinal organoid model containing M cells. a, Schematic of M cell differentiation from human intestinal organoids. Representative cell types in the cultured organoids are indicated. Images were created in BioRender. van Es, J. (2025) https://BioRender.com/xh7haut. EEC, enteroendocrine cell; TA cell, transit-amplifying cell. **b**,**c**, Representative flow cytometry analysis (**b**) and quantification of GP2$^+$ M cell percentage (**c**) in cultured M cell organoids. The effect of each M cell differentiation factor was evaluated by removing it from the M cell medium. **c**, For each tested factor, three different donors were tested. Each dot represents the mean value derived from three independent wells. Data are mean ± s.e.m. *P* values from one-way ANOVA with Dunnett's test. Ctrl, control; RA, retinoic acid. **d**,**e**, Representative confocal image (**d**) and flow cytometry analysis (**e**) of SPIB-P2A-tdTomato reporter organoids cultured in M cell medium. Mature M cells are marked by tdTomato fluorescence and GP2 antibody staining (green, arrows in **d**). Three independent experiments were performed on cells from one donor with similar results. Scale bar, 50 µm. **f**, scRNA-seq analysis of 375 cells derived from human M cell organoids. Cell clusters are visualized in uniform manifold approximation and projection (UMAP) plots and coloured by cell type (left) or by duplicate plates (right, representing two biological replicates). Cell numbers are shown in brackets below each indicated cell type. **g**, Violin plots showing the expression levels of cell-type-specific markers for M cells and enterocytes in the M cell organoid-derived scRNA-seq dataset containing 375 cells. **h**, Representative TEM images of M cell organoids. M cells are identified by having fewer apical microvilli compared with neighbouring enterocytes. M cell organoids from two donors were tested with similar results (see also Extended Data Fig. 1p). Scale bars: 10 µm (left), 2 µm (middle and right).

(IHC) staining for TFF2 on human duodenum sections stained Brunner's gland (Extended Data Fig. 1o). Exclusion of these cells defined a core set of primary human M cell markers, including *GP2*, *SPIB*, *SOX8*, *SLC2A6*, *PTAFR* and *GABRP* (Extended Data Fig. 1m), which were also highly expressed in organoid M cells (Fig. 1g). M cells exhibit far fewer and shorter apical microvilli compared with enterocytes[4,5]. Transmission electron microscopy (TEM) imaging of organoid M cells visualized this difference (Fig. 1h and Extended Data Fig. 1p). We further established a two-dimensional (2D) air–liquid interface (ALI) culture based on M cell medium (Extended Data Fig. 1q–s). Apical microvillus structures were clearly visible with actin staining, and co-staining for GP2 confirmed that cells with fewer microvilli were M cells (Extended Data Fig. 1t). We conclude that our organoid model generates genuine human M cells.

ICAM2 marks M-lineage cells

GP2 is the only known surface marker for rare, fully mature M cells[10]. The primary M cell dataset suggested *ICAM2* as a broader M cell marker

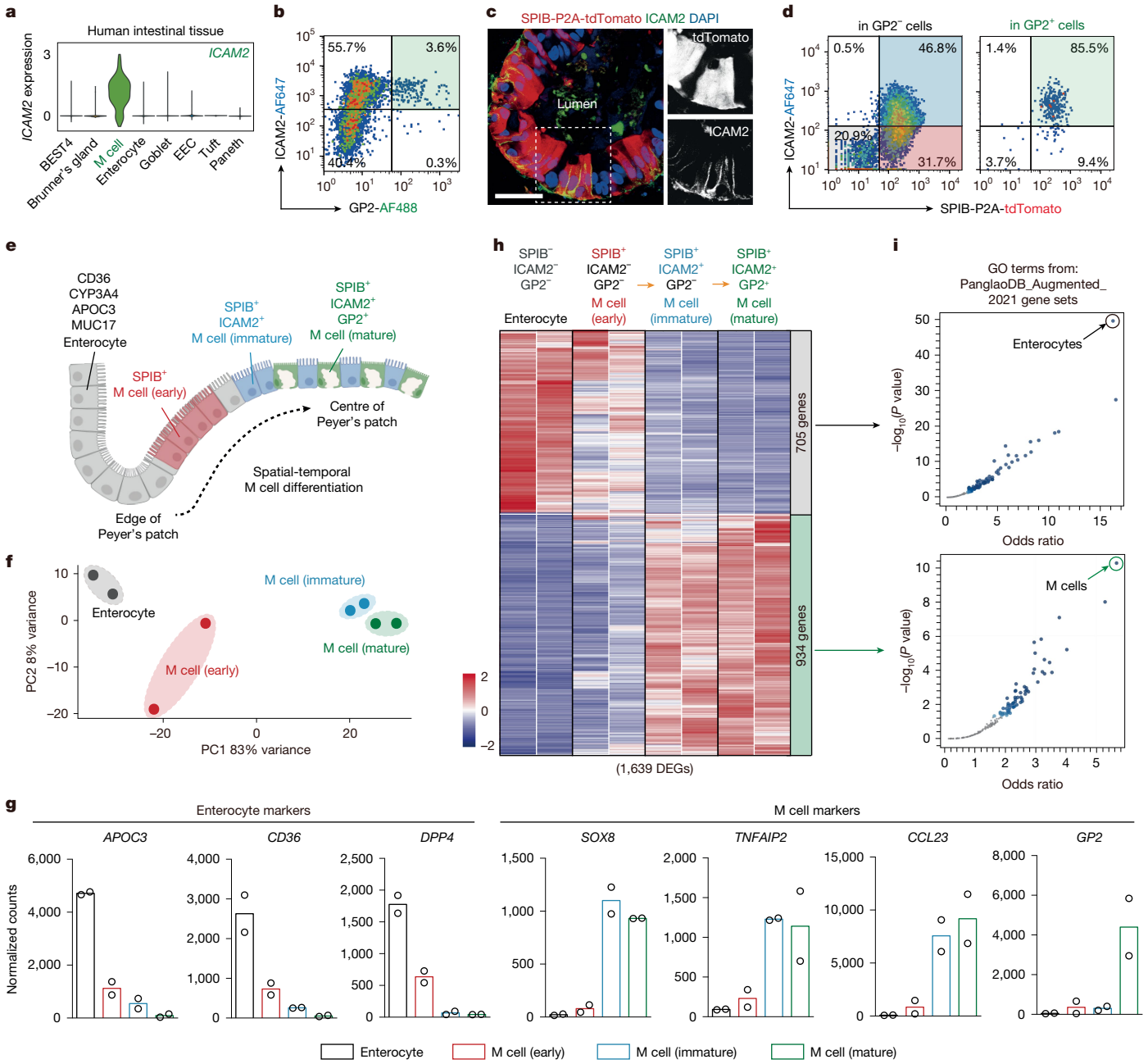

Fig. 2 | Differentiation trajectory of human M cells. a, Violin plot showing the expression levels of *ICAM2* across multiple human intestinal cell types from tissue-derived scRNA-seq datasets containing 15,543 cells. **b**, Representative flow cytometry analysis of ICAM2 and GP2 expression in M cell organoids. Three independent experiments were performed on two donors with similar results. **c**, Representative confocal images of ICAM2 antibody staining in SPIB-P2A-tdTomato reporter organoids cultured in M cell medium. M cells are marked by tdTomato fluorescence (red) and show positive staining of ICAM2 antibody (green, primarily detected on the basolateral cell surface of M cells). Three independent experiments were performed with cells from one donor with similar results. Scale bar, 50 µm. **d**, Representative flow cytometry analysis of ICAM2 and GP2 expression in SPIB-P2A-tdTomato reporter organoids cultured in M cell medium. Three independent experiments were performed on one donor with similar results. **e**, Schematic of spatial-temporal differentiation of human M cells, showing markers associated with M cells at different stages. Images were created in BioRender. van Es, J. (2025) https://BioRender.com/xh7haut. **f**, Principal components analysis plot showing transcriptomal changes during M cell differentiation. $n = 2$ biological replicates from one donor. Each dot represents one biological replicate for the FACS-sorted cell population. **g**, Expression levels (normalized counts) of cell-type-specific markers across the indicated cell populations. $n = 2$ biological replicates. Data are mean values. **h**, Heat map showing expression patterns of DEGs during M cell differentiation. $n = 2$ biological replicates. **i**, Volcano plot showing GO analysis based on downregulated and upregulated DEGs in M cells, which identifies the most relevant cell types as enterocytes and M cells, respectively. *P* values from one-sided Fisher's exact test.

(Fig. 2a). Indeed, ICAM2 was expressed in more than 90% of GP2⁺ organoid M cells (Fig. 2b), yet about 50% of GP2⁻ cells also expressed ICAM2 (Fig. 2b). SPIB⁺ M-lineage organoid cells could be subdivided into ICAM2⁻ and ICAM2⁺ cells (Fig. 2c,d). Thus, we could distinguish three stages within the M-lineage cells—SPIB⁺ICAM2⁻GP2⁻ early M cells, SPIB⁺ICAM2⁺GP2⁻ immature M cells and SPIB⁺ICAM2⁺GP2⁺ mature M cells—in addition to SPIB⁻ICAM2⁻GP2⁻ non-M cells (Fig. 2d,e). These four populations were sorted for transcriptome profiling (Fig. 2d,f). SPIB⁻ non-M cells expressed enterocyte markers that decreased in abundance during M cell differentiation (Fig. 2g and Extended

Data Fig. 2a). Immature M cell markers (*TNFAIP2* (ref. 19), *SOX8* and *CCL23*) were enriched in ICAM2$^+$ cells (Fig. 2g). M cell maturation coincided with appearance of previously reported human M cell markers and RANKL-responsive genes[16] (Extended Data Fig. 2b). In total, 1,639 differentially expressed genes (DEGs) were identified (Fig. 2h). Gene ontology (GO) analysis identified enterocytes and M cells as the most relevant cell types on the basis of the downregulated and upregulated genes in M cells, respectively (Fig. 2i). Additionally, gene set enrichment analysis (GSEA) revealed nutrient metabolic pathways and brush border components in enterocytes, whereas M cells expressed genes related to pathogen infection and immune cell interaction (Extended Data Fig. 2c–e). Markers for other intestinal cell types were undetectable in M cell organoids (Extended Data Fig. 2f). In human Peyer's patch tissues, immunofluorescent staining confirmed the presence of ICAM2$^+$ M cells (Extended Data Fig. 3a). Some ICAM2$^+$ cells exhibited features of mature M cells, yet most represented immature M cells with enterocyte-like brush borders. scRNA-seq analysis of primary M cells confirmed that early, immature and mature stages were distinguishable by *SPIB*, *ICAM2* and *GP2* expression (Extended Data Fig. 3b). GP2$^-$ and GP2$^+$ ICAM2-enriched subpopulations equally expressed immature M cell markers, such as *TNFAIP2* and *CCL23* (Extended Data Fig. 3b). Thus, organoid M cells faithfully recapitulated human M cell differentiation. Although GP2 uniquely marks mature M cells (Fig. 2g and Extended Data Fig. 3c,d), the transcriptome of ICAM2$^+$GP2$^-$ M cells strongly resembled that of GP2$^+$ M cells (Extended Data Fig. 3c,d). Only nine genes were upregulated more than twofold in GP2$^+$ cells (Extended Data Fig. 3c,d). Indeed, *CLU* is known to mark GP2$^+$ M cells[10]. The minimal transcriptomic difference was also observed in primary M cells (Extended Data Fig. 3e,f). Of note, some GP2$^-$ M cells also displayed the typical M cell microvillus morphology (Extended Data Fig. 1t, arrows).

ICAM1 and *ICAM2* are co-expressed by primary (Fig. 2a and Extended Data Fig. 3g) and organoid (Extended Data Figs. 2b and 3h) M cells. ICAM2 is located basolaterally (Fig. 2c and Extended Data Fig. 3a). ICAM molecules can facilitate adhesion between T cells and antigen-presenting cells[20]. We next analysed the role of ICAM2 in CD4$^+$ T cell binding to M cell organoids. We genetically deleted *ICAM2* (Extended Data Fig. 3i) and blocked ICAM1 with a neutralizing antibody, which resulted in decreased numbers of T cells attached to the M cell organoids (Extended Data Fig. 3j,k). Notably, *ICAM2* knockout did not affect M cell differentiation (Extended Data Fig. 3l,m).

Human M cell development requires RUNX2

Expression of 63 transcription factors increased during M cell differentiation (Extended Data Fig. 4a), including the known M cell transcription factors SPIB, SOX8, EHF[21], RELB, NFKB1 (nuclear factor (NF)-κB p105 subunit) and NFKB2 (NF-κB p100 subunit)[22] (Extended Data Fig. 4a), whereas expression of 59 transcription factors decreased. ONECUT2 drives enterocyte differentiation in mice[15]. Its expression was markedly decreased during human M cell maturation (Extended Data Fig. 4b). Treatment with the ONECUT2 inhibitor CSRM617 resulted in more than twofold increase in the number of GP2$^+$ M cells in organoids (Extended Data Fig. 4c,d). SPIB is described as a master regulator for MHC-II-expressing B cells[23] and dendritic cells[24]. *Spib* deficiency depletes GP2$^+$ M cells in mouse Peyer's patch epithelium[8]. *SPIB*-knockout organoids revealed the same essential role of SPIB in human M cell development (Extended Data Fig. 4e,f).

RANKL signalling is an essential niche factor for dendritic cell activation[25]. Several RANKL-induced M cell transcription factors, besides SPIB, are known from dendritic cell biology (that is, EHF, RELB and NFKB1/2)[26]. We hypothesized that dendritic cells and M cells might share a RANKL-induced transcription regulatory network. One transcription factor expressed by M cells, RUNX2, attracted our interest (Extended Data Fig. 4a,b). Like SPIB, RUNX2 is a master regulator for dendritic cells[27] and its expression is induced by RANKL[28]. Addition of CADD522, a RUNX2-specific inhibitor, resulted in dose-dependent loss of GP2$^+$ M cells (Extended Data Fig. 4g–i). Similarly, *RUNX2* knockout led to significant loss of GP2$^+$ organoid M cells (Extended Data Fig. 4g–j).

CSF2 promotes human M cell maturation

We next interrogated the dataset for M cell-expressed receptors (Extended Data Fig. 4k). Consistent with the functional effects of RANKL, TNF and retinoic acid, their receptors (TNFRSF11A, TNFRSF1B and RARG, respectively) were expressed in M cells (Extended Data Fig. 4k). We performed FACS-based screening to identify potential niche factors that could promote M cell maturation (Extended Data Fig. 4l,m). Among 12 tested ligands, CSF2 resulted in a more than fourfold increase of GP2$^+$ organoid M cells (Extended Data Fig. 4l–n). CSF2 is widely used for dendritic cell differentiation in vitro. The CSF2 receptor was expressed in primary human M cells, indicating its potential function in vivo (Extended Data Fig. 4o). Notably, expression of CSF2 receptors was undetectable by qPCR analysis in organoid-derived GP2$^+$ mouse M cells (Extended Data Fig. 5a,b) and was minimal in a published mouse scRNA-seq dataset containing RANKL-induced M cells[29] (Extended Data Fig. 5c), demonstrating an interspecies difference.

Human M cells express dendritic cell-related genes

The shared transcription factors (SPIB, RUNX2, RELB and NF-κB) and signalling regulators (RANKL and CSF2) between M cells and dendritic cells suggested a shared gene regulatory network. This prompted us to search for additional dendritic cell genes in our RNA-seq dataset. A series of lymphoid dendritic cell marker genes was induced during M cell maturation (Fig. 3a). Intestinal lymphoid dendritic cells have been defined by signature genes including *CD83*, *LAMP3*, *IL7R* and *FSCN1* (refs. 17,30) and resemble conventional dendritic cells (cDCs) more than plasmacytoid dendritic cells (pDCs)[30]. We integrated scRNA-seq datasets of primary human intestinal epithelial cells with various immune cell types (Extended Data Fig. 5d,e). Unsupervised, transcriptomic similarity-based clustering of individual epithelial and immune cells identified a unique cell cluster (cluster 9), in which both primary M cells and lymphoid dendritic cells resided (Extended Data Fig. 5d,e, with cell types annotated by the previous study[17]). Signature genes defining cluster 9 included the lymphoid dendritic cell markers (Extended Data Fig. 5f) and were expressed by both lymphoid dendritic cells and M cells (Fig. 3b and Extended Data Fig. 5f). Within cluster 9, M cells, but not lymphoid dendritic cells, specifically expressed conventional M cell markers including *ICAM2*, *CCL23* and *SOX8* (Extended Data Fig. 5f). Notably, although M cells clustered with lymphoid dendritic cells, a number of cDC genes (*CD74*, *DC-SIGN* and *CD11B*) and several pDC genes (*CXCR3* and *RUNX2*) also appeared upon M cell differentiation (Extended Data Fig. 5g). Thus, M cells did not resemble a specific dendritic cell subtype, but rather exhibited broader expression of dendritic cell-related genes. Finally, GO analysis using all DEGs induced during M cell maturation identified activated dendritic cells and antigen-presenting cells as being most closely related (Fig. 3c).

Human M cells express MHC-II

Dendritic cells take up exogenous antigens and process these into peptides, which are then presented by MHC-II complexes. FACS-sorted M cells exhibited distinct morphology from SPIB$^-$ cells when cultured in 2D, with multiple protrusions resembling dendritic cells (Extended Data Fig. 5h). These protrusions facilitated phagocytosis of bacteria particles (Supplementary Video), which could be blocked by the phagocytosis inhibitor cytochalasin B (Extended Data Fig. 5i,j). Notably, expression of MHC-II genes and the invariant chain (*CD74*) increased during M cell maturation (Fig. 3d and Extended Data Fig. 5k). Flow cytometry analysis for MHC-II and GP2 confirmed expression of MHC-II proteins

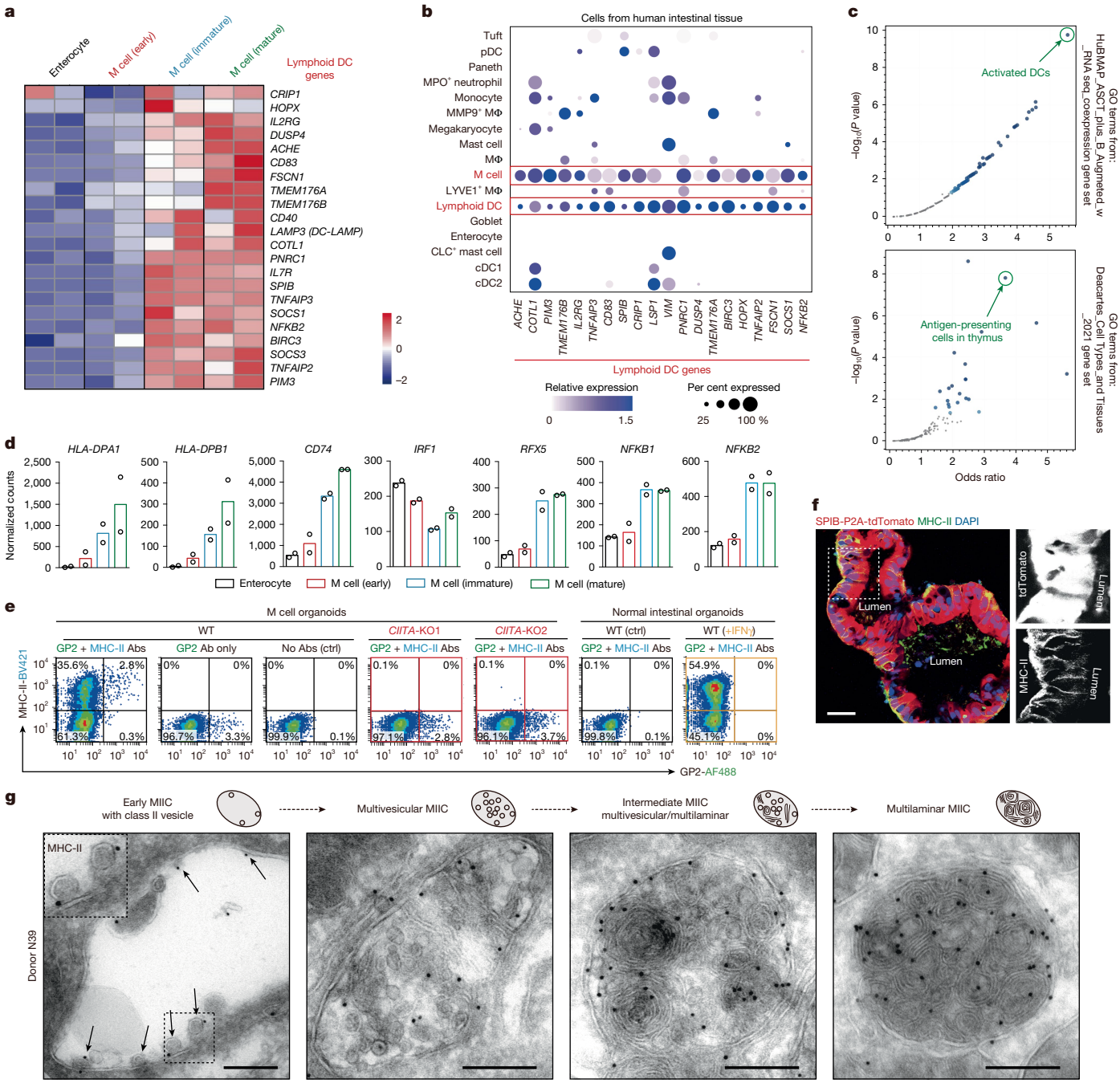

Fig. 3 | Human M cells express dendritic cell markers including MHC-II. **a**, Heat map showing the expression patterns of a set of lymphoid dendritic cell markers during M cell differentiation. $n = 2$ biological replicates. **b**, Dot plot showing the expression levels of a set of lymphoid dendritic cell markers (cluster 9 markers) across multiple intestinal epithelial and immune cell types from tissue-derived scRNA-seq datasets. $n = 20{,}210$ single cells. Dot colour relates to normalized mean expression values and dot size indicates the fraction of expressing cells. **c**, Volcano plot showing GO analysis based on upregulated DEGs in M cells, which identifies the most relevant cell types as activated dendritic cells (top) or antigen-presenting cells (bottom). *P* values from one-sided Fisher's exact test. **d**, Expression levels (normalized counts) of MHC-II-related genes across the indicated cell populations. $n = 2$ biological replicates. Data are mean values. **e**, Representative flow cytometry analysis of MHC-II and GP2 expression in cultured M cell organoids (wild type or *CIITA*-knockout (KO)) versus normal intestinal organoids (with or without IFNγ). Three independent experiments were performed with similar results in wild-type organoids derived from three donors and in two *CIITA*-knockout clonal organoid lines derived from one donor. Abs, antibodies; WT, wildtype. **f**, Representative confocal images of MHC-II antibody staining in SPIB-P2A-tdTomato reporter organoids cultured in M cell medium. M cells are marked by tdTomato fluorescence (red) and show positive staining of MHC-II antibody (green, detected in both cytoplasm and primarily on basolateral surface of M cells). Three independent experiments were performed on cells from one donor with similar results. Scale bar, 50 µm. **g**, Representative immuno-electron microscopy images showing MIIC structures in endosomes, identified by immunogold staining of MHC-II antibody in organoid M cells. Arrows indicate MHC-II vesicles in the endosome. M cell organoids from two donors were tested with similar results (see also Extended Data Fig. 8a). Scale bars, 200 nm.

on GP2$^+$ as well as GP2$^-$ M cells (Fig. 3e). Notably, MHC-II proteins were expressed by SPIB$^+$ M-lineage cells, with the staining signals primarily detected on the basolateral cell surface (Fig. 3f), whereas SPIB$^-$ cells did not express MHC-II genes (Fig. 3d). Flow cytometry analysis confirmed that MHC-II$^+$ M cells were more mature, with more than 98% of MHC-II$^+$ cells co-expressing ICAM2 (Extended Data Fig. 5l). Consistently,

FACS-sorted MHC-II$^+$ cells expressed various markers of immature and mature M cells (Extended Data Fig. 5m).

Notably, intestinal organoids cultured without M cell-inducing factors did not express MHC-II in the absence of IFNγ (Fig. 3e), as also shown elsewhere[16]. By contrast, human organoid M cells spontaneously expressed MHC-II without IFNγ under homeostatic conditions (Fig. 3e). To test whether the IFNγ-independent expression of MHC-II in M cells required the transcription factor CIITA, we generated *CIITA*-knockout organoids (Extended Data Fig. 5n). These organoids contained similar numbers of M cells, yet MHC-II expression was absent (Fig. 3e). IRF1 is the classical upstream transcription factor that induces *CIITA* expression in the presence of IFNγ. Expression of IRF1 was not induced during M cell differentiation (Fig. 3d and Extended Data Fig. 3b), indicating that *CIITA* expression in M cells does not depend on IRF1, which further confirms that MHC-II expression in M cell organoids is independent of IFNγ signalling. Beyond IRF1, several IFNγ-independent transcription factors have been reported as potential upstream regulators of *CIITA* (for example, RFX5 (ref. 31) and NF-κB[32]). These genes were induced by threefold to fivefold during M cell differentiation (Fig. 3d).

In primary intestine, MHC-II can be expressed by enterocytes[33]. The expression of MHC-II in enterocytes crucially depends on IFNγ stimulation during inflammation[33,34]. MHC-II expression is almost completely abolished in *Ifngr1*-knockout mouse enterocytes, even with pathogenic bacterial infection[34]. In human intestinal tissues, MHC-II$^+$ enterocytes were not uniformly detectable but showed different distributions between donors and tissue areas (Extended Data Fig. 6a), indicating that expression of MHC-II is not a spontaneous, intrinsic property, but is induced by exogenous factors such as IFNγ. Notably, unlike M cells, the transcriptome of MHC-II$^+$ enterocytes did not resemble that of lymphoid dendritic cells (Extended Data Fig. 6b). In the scRNA-seq datasets, MHC-II$^+$ enterocytes did not cluster with any dendritic cell subtype (Extended Data Fig. 6c). Transcriptomic comparison between MHC-II-expressing M cells and enterocytes identified 414 DEGs that were expressed at higher levels in M cells (Extended Data Fig. 6d,e). These DEGs were again highly co-related with blood dendritic cells, as revealed by GO analysis (Extended Data Fig. 6f).

It has remained controversial whether human M cells can directly present antigens to CD4$^+$ T cells[5,35,36]. We performed immunofluorescent staining of MHC-II on primary human Peyer's patch tissues. MHC-II signals could be detected intracellularly and on the basolateral cell surface of M cells (Extended Data Fig. 6g,h). Of note, scRNA-seq analysis based on reliable M cell marker genes revealed that both ICAM2$^+$GP2$^-$ and ICAM2$^+$GP2$^+$ primary M cells expressed MHC-II genes and *CD74* (Extended Data Fig. 6i). This analysis avoids limitations of IHC staining regarding the uncertainty of MHC-II signals between neighbouring cells[35,36]. Furthermore, flow cytometry analysis of MHC-II in ICAM2$^+$ or GP2$^+$ primary M cells confirmed MHC-II protein expression in more than 97% of ICAM2$^+$ and GP2$^+$ M cells (Extended Data Fig. 6j,k). Although two previous M cell studies reached contradictory conclusions regarding MHC-II expression in M cells, both detected MHC-II signals in human follicle-associated epithelium (FAE) tissues[35,36]. It should be noted that besides GP2$^+$ M cells, FAE also contains many M-lineage cells that do not express *GP2* (refs. 9,19) and morphologically resemble non-M enterocytes. In M cell organoids, many GP2$^-$ immature M cells were found to express MHC-II in the absence of IFNγ, in addition to GP2$^+$ M cells (Fig. 3e). Therefore, we hypothesized that in primary tissue, MHC-II$^+$ FAE cells (GP2$^-$ normal microvilli) are likely to represent immature M cells that constitutively express MHC-II, rather than representing IFNγ-induced MHC-II$^+$ enterocytes. Indeed, many ICAM2$^+$ immature M cells carried normal microvillus structures in human FAE (Extended Data Fig. 3a), and a majority of these primary ICAM2$^+$ M cells expressed MHC-II (Extended Data Fig. 6k). Of note, the presence of occasional MHC-II$^+$ enterocytes (induced by IFNγ) in human FAE could not be formally excluded.

Notably, MHC-II expression was not observed in mouse M cells derived either from organoids (Extended Data Fig. 5b,c) or from primary FAE tissues (Extended Data Fig. 7a–c). Most dendritic cell markers identified in human M cells were not expressed in mouse (Extended Data Fig. 5c). GO analysis of mouse M cell markers identified terms related to conventional M cell functions, but no terms related to antigen presentation (Extended Data Fig. 7d). These differences may explain why an antigen-presenting function of M cells has not been observed in mouse experiments despite clear similarities between mouse and human M cells (Extended Data Fig. 7e).

A hallmark of antigen presentation via MHC-II molecules is the MHC-II compartment (MIIC), where antigen processing and loading occur[37]. We assessed the existence of MIIC in M cells by immuno-electron microscopy imaging of MHC-II and CD63, two marker proteins for MIIC structures[37], and identified structures that represent early, multivesicular, intermediate and multilaminar MIICs in M cells and resemble the corresponding MIIC structures in dendritic cells[37,38] (Fig. 3g and Extended Data Fig. 8a). We also analysed MIIC in normal intestinal organoids. Consistent with undetectable levels of MHC-II in unstimulated normal intestinal organoids (Fig. 3e), no MHC-II$^+$ vesicles were observed in the endosomes (Extended Data Fig. 8b). Upon IFNγ stimulation, normal intestinal organoids predominantly exhibited multivesicular MIIC structures, whereas tubular extensions and the multilaminar structures were rarely observed (Extended Data Fig. 8b). Given the proposed role of multilaminar MIICs in high-fidelity peptide exchange[39], these structural differences may underlie the limited capacity for complete antigen processing and presentation by IFNγ-induced enterocytes, despite the presence of surface MHC-II. Additionally, like dendritic cells, various pattern recognition receptors and key components of the antigen processing and presentation machinery were expressed in M cells, further supporting their potential antigen-presenting function (Extended Data Fig. 8c–e).

Human M cells present gluten antigen

Next, we established an organoid/T cell co-culture assay focused on T cell activation in coeliac disease (CeD), an auto-immune disorder that is triggered by gliadin-derived antigens and linked to HLA-DQ haplotypes (HLA-DQ2.5)[40]. To our knowledge, the CeD model is the most comprehensively characterized antigen-presentation platform in the human intestine, with clearly defined HLA haplotypes, pathogenic antigen sequences and antigen-specific T cell receptor (TCR) sequences[41,42]. We synthesized a representative 33-mer antigenic peptide originated from α2-gliadin (referred to as 33-mer peptide; with sequence LQLQPF(PQPELPY)$_3$PQPQPF) and generated transgenic reporter Jurkat T cell lines expressing the specific TCR: S16 (ref. 42) or D2 (ref. 41) (Extended Data Fig. 9c).

Organoid lines were established from two HLA-DQ2.5 donors, which expressed MHC-II in M cells upon differentiation (Extended Data Fig. 9a, b). After adding the 33-mer peptide, we performed immunofluorescent staining using an antibody (DONQ52 antibody) that recognizes immunogenic gliadin peptide–HLA-DQ2.5 complexes[41]. Staining signals were detected in M cell organoids with the HLA-DQ2.5 haplotype, but not in non-HLA-DQ2.5 organoids or when the peptide was absent (Extended Data Fig. 9d). Given that MHC-II molecules are primarily located basolaterally (on the 'outside') in M cell organoids (Fig. 3f), the 33-mer peptide in culture medium could bind directly to HLA-DQ2.5 without intracellular processing. We therefore generated apical-out M cell organoids by removing the extracellular matrix, resulting in luminal localization of MHC-II (Fig. 4a). Loading the 33-mer peptide onto HLA-DQ2.5 would thus require endocytosis. Immunofluorescent staining using the DONQ52 antibody again detected gliadin peptide–HLA-DQ2.5 complexes in GP2$^+$ M cells derived from HLA-DQ2.5 donors, but not in those from non-HLA-DQ2.5 donors (Fig. 4b). HLA-DQ2.5 M cells with limited phagocytosis also exhibited

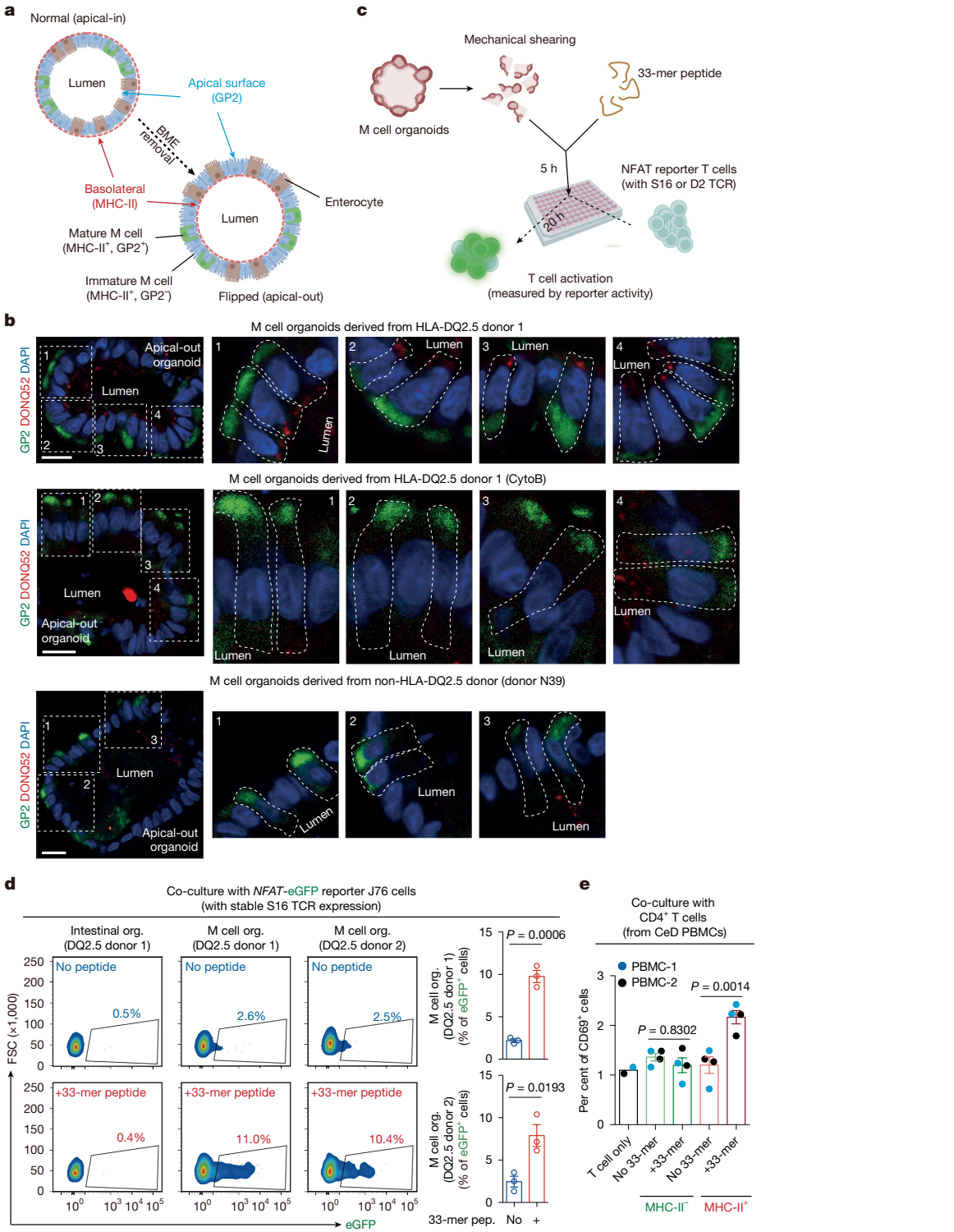

Fig. 4 | Human M cells present gluten antigen for T cell activation. a, Schematic of normal versus flipped organoids. Images were created in BioRender. van Es, J. (2025) https://BioRender.com/xh7haut. BME, basement membrane extract. **b**, Representative confocal images of DONQ52 antibody staining in apical-out M cell organoids derived from HLA-DQ2.5 and non-HLA-DQ2.5 donors. The 33-mer peptide was added before staining. M cells are marked by GP2 antibody staining (green). DONQ52 antibody specifically recognizes the gliadin peptide–HLA-DQ2.5 complexes (red). In each condition, three independent experiments were performed on cells from two donors with similar results. Scale bars, 20 µm. **c**, Schematic of organoid–T cell co-culture assay. Images were created in BioRender. van Es, J. (2025) https://BioRender.com/xh7haut. **d**, Representative flow cytometry analysis and quantification of eGFP$^+$ T cell percentage after co-culture with organoids treated with or without 33-mer peptide. Organoids (org.) from two HLA-DQ2.5 (DQ2.5) donors were tested. For each donor, $n = 3$ biological replicates are shown; each dot represents one biological replicate. Data are mean ± s.e.m. *P* values from two-tailed *t*-test. **e**, Activation of CD4$^+$ T cells derived from patients with CeD, quantified by flow cytometry analysis of CD69$^+$ cells after co-culture with MHC-II$^+$ or MHC-II$^-$ cells treated with or without 33-mer peptide. MHC-II$^+$ and MHC-II$^-$ cells were sorted by FACS from M cell organoids derived from HLA-DQ2.5 donor 2. Patient-derived T cells were isolated from peripheral blood mononuclear cells (PBMCs) from two HLA-DQ2.5 donors. For each PBMC donor, one T cell-only well and two independent co-culture wells are shown. Each dot represents one well. Data are mean values or mean ± s.e.m. *P* values from one-way ANOVA with Tukey's test.

reduced peptide–HLA-DQ2.5 signals (Fig. 4b), confirming that the peptide was taken up by M cells and loaded onto HLA-DQ2.5.

To assess the effect of M cell-presented, CeD-associated epitopes on T cell activation, we co-cultured organoids with Jurkat T cells expressing the HLA-DQ2.5-restricted, gluten peptide-specific S16 or D2 TCRs. T cell activation was measured by eGFP fluorescence or luciferase activity induced by activated NFAT (Fig. 4c and Extended Data Fig. 9c). M cell organoids treated with the 33-mer peptide efficiently activated T cells compared with untreated organoids (Fig. 4d and Extended Data Fig. 9e). By contrast, the addition of 33-mer peptide to intestinal organoids without M cells did not induce T cell activation (Fig. 4d and Extended Data Fig. 9e). We validated this in a more physiologically relevant context by co-culturing the MHC-II$^+$ and MHC-II$^-$ cells derived from HLA-DQ2.5 M cell organoids with primary CD4$^+$ T cells isolated from blood lymphocytes of patients with CeD with the HLA-DQ2.5 haplotype. Flow cytometry analysis for the T cell activation marker CD69 confirmed MHC-II-restricted, gliadin antigen-dependent T cell activation, mediated upon M cell antigen presentation (Fig. 4e).

Human M cells deamidate gliadin peptides

We next exposed apical-out M cell organoids to enzyme (pepsin, trypsin and tissue transglutaminase)-digested whole-gliadin proteins. DONQ52 antibody staining again detected gliadin peptide–HLA-DQ2.5 complexes in GP2$^+$ M cells (Fig. 5a), indicating that gliadin proteins were taken up through the apical side of M cells, processed and loaded onto HLA-DQ2.5. In co-culture assays, these gliadin protein-treated M cell organoids activated antigen-specific T cells to a level similar to that of the 33-mer peptide-treated M cell organoids (Fig. 5b).

Efficient gliadin-derived peptide loading onto HLA-DQ2.5 requires deamidation: glutamine (Q) is converted to glutamic acid (E) in the original gliadin peptides[43] (Fig. 5c). The responsible enzyme, TGM2, has been reported to be predominantly expressed by intestinal stromal cells residing on the basolateral side of gut epithelium[44], and its expression can be upregulated by RANKL[45]. Of note, M cells highly expressed TGM2 to levels more than 18-fold higher than in enterocytes (Fig. 5d). Thus, M cells may convert the original gliadin peptides into the pathogenic peptides. We added the 33-mer peptide (Q) without the Q-to-E conversion (Fig. 5c) to M cell organoids, which resulted in T cell activation (Fig. 5e). This T cell activation by 33-mer peptide (Q) could be blocked by ZED1227, a TGM2-specific inhibitor (Fig. 5e). DONQ52 antibody staining confirmed that enzyme (pepsin and trypsin, but without tissue transglutaminase)-digested gliadin proteins were processed and efficiently loaded onto HLA-DQ2.5 (Fig. 5f). This implied Q-to-E conversion of the gliadin protein-derived peptides by M cell-derived TGM2. To further validate this, we generated *TGM2*-knockout organoids (Fig. 5g). Absence of TGM2 protein in M cell organoids and the culture medium was validated by ELISA (Extended Data Fig. 9f). Knockout of *TGM2* did not affect M cell differentiation and MHC-II expression (Fig. 5h). Thus, the 33-mer peptide (Q to E) and TGM2-treated gliadin proteins could still be presented by HLA-DQ2.5 on the *TGM2*-knockout organoids as read out in the reporter T cell activation assays (Fig. 5i). The 33-mer peptide (Q) and gliadin proteins (the latter not treated with TGM2) did not activate the reporter T cells (Fig. 5i). This was consistent with a previous report that found that D2 TCR activation depends on the presence of E residue in the gliadin-derived epitopes[41]. In addition, *SPIB*-knockout organoids did not activate the reporter T cells in co-culture assays when using 33-mer peptide (Q) and gliadin proteins without TGM2 treatment as antigens (Extended Data Fig. 9g), confirming the essential role of M cells and M cell-derived TGM2 in T cell activation. Notably, compared with M cells, IFNγ-induced MHC-II$^+$ enterocytes exhibited significantly lower efficiency in activating reporter T cells in organoid–T cell co-culture assays with TGM2-treated gliadin proteins as antigens (Extended Data Fig. 9h). These observations implied that human M cells directly take up wheat-derived gliadin proteins from the gut lumen and process these into CeD-associated peptides for HLA-DQ2.5 loading, to subsequently activate T cells.

To generalize our findings on M cell-mediated antigen presentation, we sought another defined antigen-based approach. We used a previously described[46] human-specific antigen cocktail, presented by MHC-II molecules. Adding this antigen cocktail in co-cultured M cells and autologous primary naive CD4$^+$ T cells resulted in MHC-II-restricted, antigen-dependent naive CD4$^+$ T cell activation by M cells (Extended Data Fig. 10a). In addition to the antigen cocktail, we incorporated CytoStim, an antibody-based reagent that was previously used to demonstrate antigen-presenting function in human HSPCs[46]. This approach reveals the intrinsic capacity to trigger activation and proliferation in a system that bypasses the constraints of peptide specificity and donor matching. Flow cytometry analysis of the co-cultured naive T cells demonstrated robust upregulation of CD69 and significant T cell proliferation, both occurring in an MHC-II-restricted, CytoStim-dependent manner (Extended Data Fig. 10b). Notably, the activation levels (as indicated by CD69 expression levels) of naive CD4$^+$ T cells induced by CytoStim are higher than those induced by the antigen cocktail (Extended Data Fig. 10a). Although we observed a significant increase in CD69$^+$ cells with the antigen cocktail, these CD69$^+$ cells probably included T cells with suboptimal activation (Extended Data Fig. 10a). Together, these results provided functional evidence that M cell-mediated antigen presentation can induce naive T cell activation and proliferation.

Effective activation of naive T cells by professional antigen-presenting cells requires co-stimulatory molecules, particularly CD80 and CD86. Although the expression levels remained modest, M cell organoids showed increased expression of these co-stimulatory molecules compared with normal intestinal organoids (Extended Data Fig. 10c). Notably, these genes could be significantly induced in M cells by immunological stimuli, such as IFNγ (Extended Data Fig. 10d), similar to what has been reported in dendritic cells, suggesting that M cells may exhibit dendritic cell-like co-stimulatory potential. By contrast, IFNγ treatment only upregulated CD40 expression but did not induce the expression of CD80 and CD86 in normal intestinal organoids (Extended Data Fig. 10d). In line with these gene expression results, IFNγ-induced MHC-II$^+$ enterocytes, when using CytoStim for co-culture assays, exhibited significantly lower efficiency than MHC-II$^+$ M cells in inducing naive T cell proliferation (Extended Data Fig. 10e), again demonstrating the superior capacity of M cells to promote CD4$^+$ T cell activation.

Discussion

Our findings reveal that human M cells share substantial similarities with dendritic cells and function as professional, yet non-haematopoietic, antigen-presenting cells. Mouse M cells do not express MHC-II. Thus, M cell-mediated antigen presentation may be unique to the human gut. Notably, the conventional role of M cells in inducing gut immune responses through transcytosis is well supported by studies in mouse and human systems. MHC-II-expressing M cells differ significantly from these previously described MHC-II$^+$ enterocytes regarding their IFNγ independency and capacity to provide the full spectrum of signals required for efficient CD4$^+$ T cell activation. Given the limited microbial exposure and low levels of IFNγ in the fetal and neonatal gut, M cells may act as early antigen-presenting cells in intestinal epithelium via constitutive MHC-II expression. This interaction could contribute to early mucosal immune education during intestinal development. M cells reside uniquely in gut-associated lymphoid tissues, where the most active epithelium–immune interactions occur. By contrast, enterocytes are not associated with lymphoid structures and, with their dense brush borders, are unlikely to sample antigens but rather are specialized to transport small sugars, amino acids, short peptides and lipids.

A previous study has reported that IFNγ-stimulated enterocytes can present CeD peptides for CD4$^+$ T cell activation. However, the T cells and IFNγ-stimulated enterocytes involved in the co-culture assay are derived

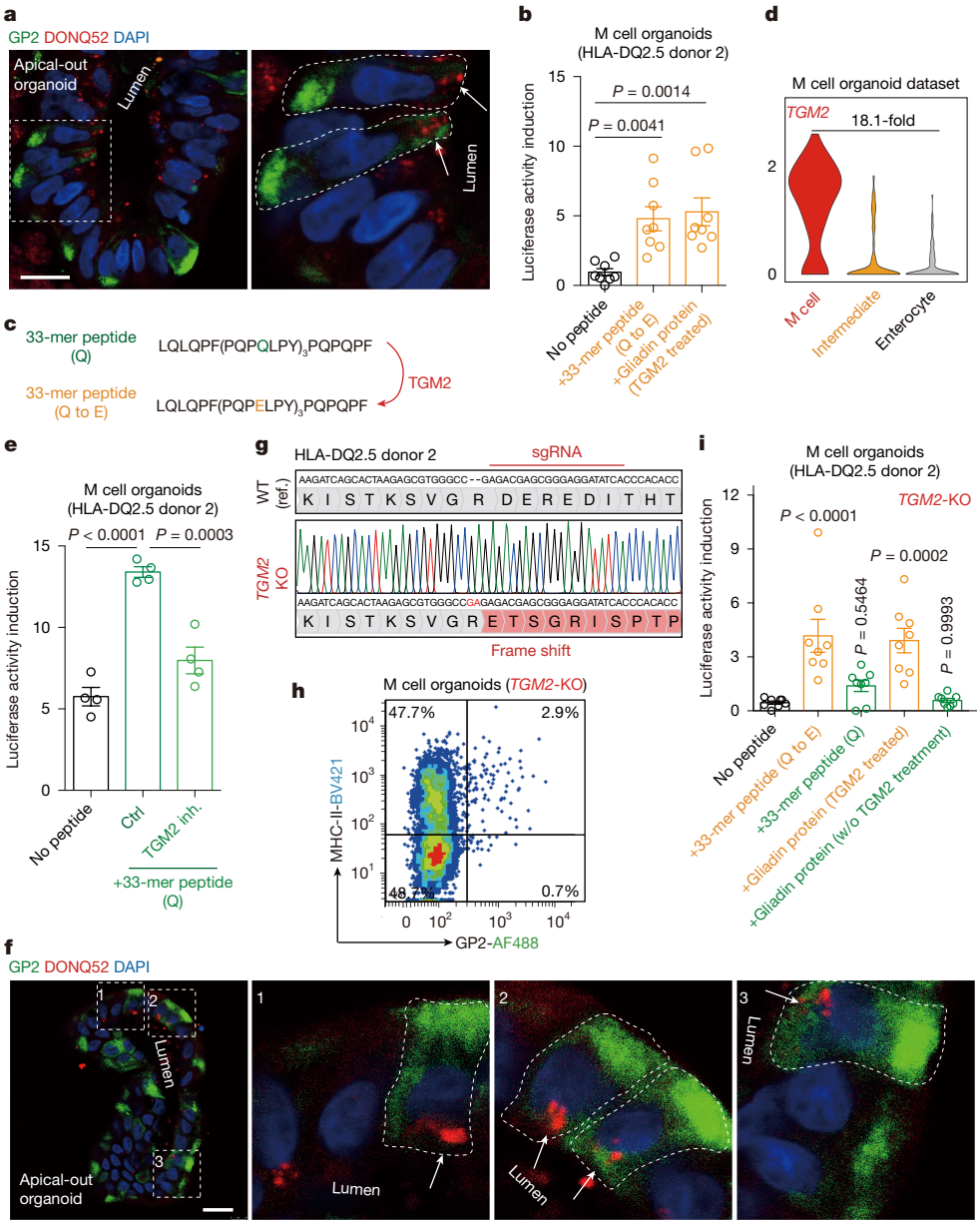

Fig. 5 | Conversion of gliadin peptide to pathogenic CeD antigen by M cell-derived TGM2. a, Representative confocal images of DONQ52 antibody staining (red) in apical-out M cell organoids treated with gliadin proteins that were pre-treated with pepsin, trypsin and TGM2. M cells are marked by GP2 antibody staining (green). Three independent experiments were performed on two HLA-DQ2.5 donors with similar results. Scale bar, 20 µm. **b**, Quantification of luciferase activity in reporter T cells co-cultured with M cell organoids treated with or without indicated peptides. $n = 8$ biological replicates on one donor. Data are mean ± s.e.m. *P* values from one-way ANOVA with Dunnett's test. **c**, Amino acid sequences showing TGM2-mediated pathogenic conversions from glutamine (Q) to glutamic acid (E) in 33-mer peptide. **d**, Violin plot showing the expression levels of *TGM2* in the M cell organoid-derived scRNA-seq dataset containing 375 cells. **e**, Quantification of luciferase activity in reporter T cells co-cultured with M cell organoids treated with or without 33-mer peptide (Q). $n = 4$ biological replicates from one donor. Data are mean ± s.e.m. *P* values from one-way ANOVA with Dunnett's test. **f**, Representative confocal images of DONQ52 antibody staining (red) in apical-out M cell organoids treated with gliadin proteins that were digested with pepsin and trypsin. M cells are marked by GP2 antibody staining (green). Three independent experiments are performed on two HLA-DQ2.5 donors with similar results. Scale bar, 20 µm. **g**, Validation of *TGM2* knockout by targeted genotyping. sgRNA, single guide RNA. **h**, Representative flow cytometry analysis of MHC-II and GP2 expression in *TGM2*-knockout M cell organoids. Three independent experiments were performed with cells from one donor with similar results. Ref., reference. **i**, Quantification of luciferase activity in reporter T cells co-cultured with *TGM2*-knockout M cell organoids treated with or without indicated peptides. $n = 8$ biological replicates from one donor. Data are mean ± s.e.m. *P* values from one-way ANOVA with Dunnett's test.

from humanized mouse models, and the transwell-based co-culture system does not support direct epithelial–immune cell interactions[47]. M cells express *TGM2* at much higher levels than enterocytes. Rahmani et al.[47] only use deamidated gliadin in their co-culture assays, which bypasses TGM2 requirement. In another recently published 2D CeD organoid model[48], Santos et al. also apply the modified gliadin peptide, rather than native gliadin protein. Of note, their organoid model does not contain M cells. We analysed the expression of 58 CeD-associated gene alleles identified by a genome-wide association study of 4,533 individuals with CeD[49]. Eight of these genes—all of which are known to be expressed by immune cells—are highly expressed in human M cells. Among these eight genes, *SOCS1*, *CLEC16A*, *ETS1* and *RUNX3* are the most prominent in the genome-wide association study (Extended Data Fig. 10f). Furthermore, IL-7 and IL-15, whose receptors are highly

expressed by M cells (Extended Data Fig. 4k), have been previously implicated in the pathogenesis of CeD[48,50]. Future studies on CeD may investigate the potential roles of these genes in M cells. It is also unclear whether and how naive T cells would migrate to Peyer's patches without previous priming, which typically occurs in gut-draining lymph nodes. One possibility is that cDCs initially prime the T cells, after which M cells further stimulate them to acquire pathogenic effector functions. Although the organoid platform offers experimental advantages over in vivo studies, it remains a reductionist system and the contribution of human M cells to gliadin-specific T cell activation in CeD, as experimentally tested in organoid system, awaits in vivo validation. Another limitation is that TGM2 was detectable in the culture medium at very low level. We cannot definitively demonstrate that gluten peptide deamidation occurs within M cells. Our findings propose a role of M cell-mediated antigen presentation in modulating intestinal immune responses, tolerance and immunological disorders.

Online content

Any methods, additional references, Nature Portfolio reporting summaries, source data, extended data, supplementary information, acknowledgements, peer review information; details of author contributions and competing interests; and statements of data and code availability are available at https://doi.org/10.1038/s41586-025-09829-8.

1. Kraehenbuhl, J.-P. & Neutra, M. R. Epithelial M cells: differentiation and function. *Annu. Rev. Cell Dev. Biol.* **16**, 301–332 (2000).
2. Kanaya, T., Williams, I. R. & Ohno, H. Intestinal M cells: tireless samplers of enteric microbiota. *Traffic* **21**, 34–44 (2019).
3. Mabbott, N. A., Donaldson, D. S., Ohno, H., Williams, I. R. & Mahajan, A. Microfold (M) cells: important immunosurveillance posts in the intestinal epithelium. *Mucosal Immunol.* **6**, 666–677 (2013).
4. Uchida, J. Electron microscopic study of microfold cells (M cells) in normal and inflamed human appendix. *Gastroenterol. Jpn.* **23**, 251–262 (1988).
5. Miller, H., Zhang, J., Kuolee, R., Patel, G. B. & Chen, W. Intestinal M cells: the fallible sentinels?. *World J. Gastroenterol.* **13**, 1477–1486 (2007).
6. de Lau, W. et al. Peyer's Patch M cells derived from $Lgr5^+$ stem cells require SpiB and are induced by RankL in cultured "miniguts". *Mol. Cell. Biol.* **32**, 3639–3647 (2012).
7. Knoop, K. A. et al. RANKL is necessary and sufficient to initiate development of antigen-sampling M cells in the intestinal epithelium. *J. Immunol.* **183**, 5738–5747 (2009).
8. Kanaya, T. et al. The Ets transcription factor Spi-B is essential for the differentiation of intestinal microfold cells. *Nat. Immunol.* **13**, 729–736 (2012).
9. Kimura, S. et al. Sox8 is essential for M cell maturation to accelerate IgA response at the early stage after weaning in mice. *J. Exp. Med.* **216**, 831–846 (2019).
10. Hase, K. et al. Uptake through glycoprotein 2 of $FimH^+$ bacteria by M cells initiates mucosal immune response. *Nature* **462**, 226–230 (2009).
11. Sharma, R., van Damme, E. J. M., Peumans, W. J., Sarsfield, P. & Schumacher, U. Lectin binding reveals divergent carbohydrate expression in human and mouse Peyer's patches. *Histochem. Cell Biol.* **105**, 459–465 (1996).
12. Giannasca, P. J., Giannasca, K. T., Leichtner, A. M. & Neutra, M. R. Human intestinal M cells display the sialyl Lewis A antigen. *Infect. Immun.* **67**, 946–953 (1999).
13. Bjerke, K., Brandtzaeg, P. & Fausa, O. T cell distribution is different in follicle-associated epithelium of human Peyer's patches and villous epithelium. *Clin. Exp. Immunol.* **74**, 270–275 (1988).
14. He, G.-W. et al. Optimized human intestinal organoid model reveals interleukin-22-dependency of paneth cell formation. *Cell Stem Cell* **29**, 1333–1345.e6 (2022).
15. Luna Velez, M. V. et al. ONECUT2 regulates RANKL-dependent enterocyte and microfold cell differentiation in the small intestine; a multi-omics study. *Nucleic Acids Res.* **51**, 1277–1296 (2023).
16. Ding, S. et al. Retinoic acid and lymphotoxin signaling promote differentiation of human intestinal M cells. *Gastroenterology* **159**, 214–226.e1 (2020).
17. Elmentaite, R. et al. Cells of the human intestinal tract mapped across space and time. *Nature* **597**, 250–255 (2021).
18. Roggenbuck, D. et al. Human glycoprotein-2 expressed in Brunner glands—a putative autoimmune target and link between Crohn's and coeliac disease. *Clin. Immunol.* **247**, 109214 (2023).
19. Kimura, S. et al. Visualization of the entire differentiation process of murine M cells: suppression of their maturation in cecal patches. *Mucosal Immunol.* **8**, 650–660 (2015).
20. Binnerts, M. E., van Kooyk, Y., Simmons, D. L. & Figdor, C. G. Distinct binding of T lymphocytes to ICAM-1, -2 or -3 upon activation of LFA-1. *Eur. J. Immunol.* **24**, 2155–2160 (2005).
21. Asai, T. & Morrison, S. L. The SRC family tyrosine kinase HCK and the ETS family transcription factors SPIB and EHF regulate transcytosis across a human follicle-associated epithelium model. *J. Biol. Chem.* **288**, 10395–10405 (2013).
22. Kanaya, T. et al. Development of intestinal M cells and follicle-associated epithelium is regulated by TRAF6-mediated NF-κB signaling. *J. Exp. Med.* **215**, 501–519 (2018).
23. Su, G. H. et al. The Ets protein Spi-B is expressed exclusively in B cells and T cells during development. *J. Exp. Med.* **184**, 203–214 (1996).
24. Sasaki, I. et al. Spi-B is critical for plasmacytoid dendritic cell function and development. *Blood* **120**, 4733–4743 (2012).
25. Anderson, D. M. et al. A homologue of the TNF receptor and its ligand enhance T-cell growth and dendritic-cell function. *Nature* **390**, 175–179 (1997).
26. Lin, Q. et al. Epigenetic program and transcription factor circuitry of dendritic cell development. *Nucleic Acids Res.* **43**, 9680–9693 (2015).
27. Sawai, C. M. et al. Transcription factor Runx2 controls the development and migration of plasmacytoid dendritic cells. *J. Exp. Med.* **210**, 2151–2159 (2013).
28. Li, S.-J. et al. Melatonin inhibits NF-κB/CREB/Runx2 signaling and alleviates aortic valve calcification. *Front. Cardiovasc. Med.* https://doi.org/10.3389/fcvm.2022.885293 (2022).
29. Haber, A. L. et al. A single-cell survey of the small intestinal epithelium. *Nature* **551**, 333–339 (2017).
30. James, K. R. et al. Distinct microbial and immune niches of the human colon. *Nat. Immunol.* **21**, 343–353 (2020).
31. Gobin, S. J. P. et al. The RFX complex is crucial for the constitutive and CIITA-mediated transactivation of MHC class I and beta2-microglobulin genes. *Immunity* **9**, 534–541 (1998).
32. Wong, D. et al. Genomic mapping of the MHC transactivator CIITA using an integrated ChIP-seq and genetical genomics approach. *Genome Biol.* **15**, 494 (2014).
33. Heuberger, C. E. et al. MHC class II antigen presentation by intestinal epithelial cells fine-tunes bacteria-reactive CD4 T-cell responses. *Mucosal Immunol.* **17**, 416–430 (2024).
34. Malik, A. et al. Epithelial IFNγ signalling and compartmentalized antigen presentation orchestrate gut immunity. *Nature* **623**, 1044–1052 (2023).
35. Bjerke, K. & Brandtzaeg, P. Lack of relation between expression of HLA-DR and secretory component (SC) in follicle-associated epithelium of human Peyer's patches. *Clin. Exp. Immunol.* **71**, 502–507 (1988).
36. Nagura, H., Ohtani, H., Masuda, T., Kimura, M. & Nakarmura, S. HLA-DR expression on M cells overlying Peyer's patches is a common feature of human small intestine. *Acta Pathol Jpn.* **41**, 818–823 (1991).
37. Geuze, H. J. The role of endosomes and lysosomes in MHC class II functioning. *Immunol. Today* **19**, 282–287 (1998).
38. van Niel, G., Wubbolts, R. & Stoorvogel, W. Endosomal sorting of MHC class II determines antigen presentation by dendritic cells. *Curr. Opin. Cell Biol.* **20**, 437–444 (2008).
39. Stern, L. J., Potolicchio, I. & Santambrogio, L. MHC class II compartment subtypes: structure and function. *Curr. Opin. Immunol.* **18**, 64–69 (2006).
40. Iversen, R. & Sollid, L. M. The immunobiology and pathogenesis of celiac disease. *Annu. Rev. Pathol.* **24**, 47–70 (2023).
41. Okura, Y. et al. Characterizations of a neutralizing antibody broadly reactive to multiple gluten peptide:HLA-DQ2.5 complexes in the context of celiac disease. *Nat. Commun.* **14**, 8502 (2023).
42. Petersen, J. et al. T-cell receptor recognition of HLA-DQ2–gliadin complexes associated with celiac disease. *Nat. Struct. Mol. Biol.* **21**, 480–488 (2014).
43. Arentz-Hansen, H. et al. The intestinal T cell response to α-gliadin in adult celiac disease is focused on a single deamidated glutamine targeted by tissue transglutaminase. *J. Exp. Med.* **191**, 603–612 (2000).
44. Granito, A., Amundsen, S. F., Stamnaes, J., Lundin, K. E. A. & Sollid, L. M. Expression of transglutaminase 2 in human gut epithelial cells: implications for coeliac disease. *PLoS ONE* **18**, e0287662 (2023).
45. Matarese, G. et al. Transglutaminase 2 up-regulation is associated with RANKL/OPG pathway in cultured HPDL cells and THP-1-differentiated macrophages. *Amino Acids* **47**, 2447–2455 (2015).
46. Hernández-Malmierca, P. et al. Antigen presentation safeguards the integrity of the hematopoietic stem cell pool. *Cell Stem Cell* **29**, 760–775.e10 (2022).
47. Rahmani, S. et al. Gluten-dependent activation of $CD4^+$ T cells by MHC class II-expressing epithelium. *Gastroenterology* **167**, 1113–1128 (2024).
48. Santos, A. J. M. et al. A human autoimmune organoid model reveals IL-7 function in coeliac disease. *Nature* **632**, 401–410 (2024).
49. Dubois, P. C. A. et al. Multiple common variants for celiac disease influencing immune gene expression. *Nat. Genet.* **42**, 295–302 (2010).
50. Abadie, V. R. et al. IL-15, gluten and HLA-DQ8 drive tissue destruction in coeliac disease. *Nature* **578**, 600–604 (2020).

Methods

Human specimens and organoid lines

Two terminal ileum tissues (donors H0514 and H0515-2) were obtained for immunofluorescent staining and flow cytometry analysis from Diakonessen Hospital Utrecht, with approval by the Medical Ethical Committee of the hospital and with informed consent of each patient.

The PBMCs from patients with CeD were collected from participants of the CeDNN study. CeDNN was approved by the Medical Ethical Committee of the University Medical Center Groningen, with METc no. 2013/440. Written consent was signed by all participants, their parents or legal representatives for participants aged under 16 for CeDNN. Normal PBMCs were purchased from Sanquin, with a signed material transfer agreement.

A total of five human intestinal organoid lines were established in our laboratory and recruited to this study. Three ileum tissues (donor 12339, 4280N/HLA-DQ2.5 #1 and 4403N/HLA-DQ2.5 #2) were obtained from the Netherlands Cancer Institute (NKI); one ileum tissue (donor N39) and one colon tissue (donor P11N) were obtained from the Diakonessen Hospital Utrecht, all with approval by the Medical Ethical Committee of the respective organizations and with informed consent of each patient.

This study was approved by the Ethical Committee of Hubrecht Institute and was in accordance with the Declaration of Helsinki and according to the Dutch law. The study complied with all relevant guidelines and regulations regarding research involving human participants.

Mice

Wild-type C57BL/6 mice were used in this study. Both male (n = 2) and female (n = 8) mice (more than 8 weeks of age) were included. No specific sample size was chosen, and neither randomization nor blinding were necessary, as no comparison was made. No specific ethical guidance was required. In this study, we only collected the intestinal Peyer's patch tissues from euthanized mice for flow cytometry analysis and immunofluorescent staining, which was approved by the Institutional Review Board of Hubrecht Institute.

Organoid culture and M cell differentiation

Human intestinal organoid culture. Three-dimensional cultured human intestinal organoids were mixed with BME (R&D Systems, 3536-005-02), seeded as ~5 µl droplets, cultured in optimized culture of human intestinal organoids (OCHIO) medium and passaged weekly through mechanical dissociation as per the method previously described[14].

M cell differentiation. To generate human M cell organoids, a differentiation cocktail including 100 ng ml^{-1} RANKL (Peprotech, 310-01 C), 20 ng ml^{-1} TNF (Peprotech, 300-01 A) and 0.1 µM retinoic acid (Sigma-Aldrich, R2625) was added into the OCHIO medium three days post-passaging. The differentiation process was typically achieved within 5–8 days.

Apical-out organoids. To release cultured organoids from BME, ice-cold Corning Cell Recovery Solution (Sigma-Aldrich, CLS354253) was used. Following the release, M cell organoids underwent a polarity change through an overnight suspension culture in M cell medium with 3 µM CHIR99021 (Tocris, 4423). Gliadin proteins or 33-mer peptides were then added for 5 h prior to immunostaining.

Two-dimensional ALI culture. Human intestinal organoids cultured in OCHIO medium were dissociated using 1 ml TripLE (TrypLE Express Enzyme, Thermo Fisher, 12605010) at 37 °C for 6–8 min, followed by gentle pipetting (20 times) to ensure thorough dissociation. The resulting cell suspension was passed through a 40-µm cell strainer and washed twice with 15 ml wash medium. The wash medium consisted of adDMEM/F12 (advanced Dulbecco's Modified Eagle's Medium/F12, Gibco, 12634028) supplemented with 100 U ml^{-1} penicillin/streptomycin (Gibco, 15140122), 10 mM HEPES (Gibco, 15630056) and 1× Glutamax (Gibco, 35050038). Post-wash, cells were resuspended with OCHIO medium and seeded into the transwell inserts (Greiner, 662641) precoated with 10% BME. OCHIO medium was added to the apical (top) and basolateral (bottom) chambers, and cells were cultured for two days. After this period, unattached cells were removed, and the remaining attached cells were cultured for an additional two days until complete confluency was achieved. To induce M cell differentiation, the OCHIO medium was removed from both chambers, and M cell differentiation medium was added only to the bottom chamber to establish an ALI system. M cell differentiation was carried out for six to eight days.

Mouse intestinal organoid culture and differentiation. The protocol is similar to the human organoid cell culture and differentiation protocol with only minor modification. Instead of OCHIO medium, we used ENR medium for mouse organoid culture[51]. ENR medium consisted of adDMEM/F12 supplemented with 100 U ml^{-1} penicillin/streptomycin, 10 mM HEPES, 1× Glutamax, 1× B-27 supplement (Thermo Fisher, 12587010), 2.5 mM *N*-acetyl-L-cysteine (Sigma-Aldrich, A9165), 0.25% (v/v) recombinant Noggin (U-Protein Express BV, Custom order), 50 ng ml^{-1} EGF (Epidermal Growth Factor, Peprotech, AF-100-15), 10 mM NIC (Nicotinamide, Sigma-Aldrich, N0636) and 0.5% (v/v) R-spondin3 (U-Protein Express BV, Custom order).

Other immune factors and molecules used in this study. LTB (Lymphotoxin α2/β1, R&D system, 679-TX-010/CF) was tested at 100 ng ml^{-1}, the same concentration as previously reported[16]. Cytokines were all from Peprotech with the following catalogue numbers: IL-2, 200-02; IL-3, 200-03; IL-4, 200-04; IL-5, 200-05; IL-7, 200-07; IL-15, 200-15; IFNα, 300-02AA; IFNγ, 300-02; MIF, 300-69; CX3CL1, 300-31; CSF2, 300-03. In the cytokine screening experiment shown in Extended Data Fig. 4l,m, interleukins, interferons, CX3CL1, MIF and CSF2 were used at 10 ng ml^{-1}. Lipopolysaccharide (Sigma-Aldrich, L4391) was used at 100 ng ml^{-1}. The concentrations of these immune factors were previously tested by us in organoid systems[14,52], which are effective without significantly affecting organoid viability. Effect of CSF2 on M cell differentiation was further tested at higher concentrations (20 ng ml^{-1} and 50 ng ml^{-1}) in organoids derived from unrelated donors. CADD522 (Selleck, S0790) was used at different titrated concentrations from 1 nM to 1 µM, and 100 nM of CADD522 was further used for validation in organoids derived from unrelated donors. CSRM617 (Sigma-Aldrich, SRL2608) was used at 50 µM. The TGM2 inhibitor ZED1227 (MedChemExpress, HY-19359) was used at 200 nM in co-culture assays and added 2 h before the peptide treatment.

Genetically modified organoids generated by CRISPR

Preparation of cells for electroporation: organoids were cultured in stem cell expansion medium[53] for 4–5 days and then dissociated into small cell clumps with 1 ml TripLE at 37 °C for 4 min, followed by gentle pipetting (20 times). The dissociated cell suspension was filtered through a 40-µm cell strainer, washed twice with cold Opti-MEM (Thermo Fisher, 31985070) and resuspended in Opti-MEM for electroporation. The expansion medium consisted of adDMEM/F12 supplemented with 100 U ml^{-1} penicillin/streptomycin, 10 mM HEPES, 1× Glutamax, 1× B-27 supplement, 1.25 mM *N*-acetyl-L-cysteine, 10 mM NIC, 1% (v/v) recombinant Noggin, 0.5 nM WNT surrogate (U-Protein Express BV, Custom order), 50 ng ml^{-1} EGF, 0.5 µM A83-01 (Tocris, 2939), 20% (v/v) RSPO1, 1 µM SB202190 (Sigma-Aldrich, S7067) and 1 µM PGE2 (Prostaglandin E2, Tocris, 2296).

sgRNAs targeting different genes were cloned into pSPgRNA vector (Addgene plasmid #47108) according to the previously described protocol[54]. The sgRNA sequences used in this study are listed in Supplementary Table 1.

SPIB-P2A-tdTomato knock-in reporter organoids[52] were generated using the CRISPR-HOT method as described[55,56].

SPIB[52], *CIITA*, *RUNX2* and *ICAM2*-knockout organoids were generated by CRISPR-mediated C-to-T base-editing[57]. Four plasmids were co-transfected into organoid cells via electroporation: a C-to-T base editor (Addgene plasmid #112100 for NGG or #125615 for NGN), a plasmid encoding a gene-specific knockout sgRNA, and a two-plasmid transposon system[58] (designed to introduce hygromycin resistance for selection). Three days post-electroporation, live single cells were sorted by FACS, based on the negative staining of DAPI (Sigma-Aldrich, 10236276001). The sorted cells were then cultured in expansion medium supplemented with hygromycin to select successfully transfected cells. Single-cell-derived subclones were subsequently hand-picked and expanded. Successful knockout organoids were confirmed by targeted genotyping via Sanger sequencing.

TGM2-knockout organoids were generated by the conventional CRISPR knockout method[59]. Four plasmids were co-transfected into organoid cells via electroporation: a frame selector plasmid (Addgene plasmid #66940), a plasmid encoding a *TGM2*-specific knockout sgRNA, and the two-plasmid transposon system. Three days post-electroporation, organoid cells were FACS-sorted based on the mCherry fluorescence. The sorted cells were then cultured in expansion medium supplemented with hygromycin. Single cell-derived subclones were subsequently hand-picked and expanded. Successful knockout organoids were confirmed by targeted genotyping via Sanger sequencing.

Immunostaining and imaging

Before fixation, organoids were released from BME using ice-cold Corning Cell Recovery Solution and primary tissues were dissected to remove the muscle layers. Then, primary tissues or organoids were fixed in 4% formaldehyde solution at 4 °C for 18 h or room temperature for 1 h, respectively, and washed three times with PBS (phosphate-buffered saline) and then embedded into OCT for cryosectioning. For immunofluorescence staining, the cryosections were blocked at room temperature for 1 h, using a blocking buffer containing 10% FBS (fetal bovine serum) in PBS-T (PBS with 0.1% Triton X-100). Primary antibodies, diluted in blocking buffer, were applied and incubated overnight at 4 °C. The sections were subsequently washed three times with PBS-T, followed by incubation with secondary antibodies overnight at 4 °C. After three additional washes with PBS-T, sections were mounted for imaging. For whole-mount immunostaining in transwell inserts, the same fixation and staining protocol were used as described above. However, instead of mounting, the transwell inserts were submerged in PBS-T, put in the glass-bottom well plate, and directly staged on the microscope for imaging. All the images were captured using a Leica SP8 confocal detection system integrated with a Leica DMi8 microscope. Leica LAS X software (v.3.5.7.23225) was used for image processing and export.

Primary antibodies used in this study: mouse anti-human GP2 (MBL, D277-3, clone 3G7-H9, diluted 1:200); mouse anti-human ICAM2 (Thermo Fisher, BMS109BT, clone CBR-IC2/2, diluted 1:200); mouse anti-human HLA-DP/DQ/DR (Thermo Fisher, MA1-25914, clone CR3/43, diluted 1:200); rat anti-mouse MHC-II (I-A/I-E) (Thermo Fisher, 14-5321-82, clone M5/114.15.2, diluted 1:200), UEA-1-Rhodamine (Vector, RL-1062-2, diluted 1:1,000); Phalloidin (Sigma, 65906-10NMOL, diluted 1:1,000); DONQ52 antibody (provided by Chugai Pharmaceutical, diluted 1:100).

IHC staining images using TFF2 and MHC-II antibodies in primary human intestinal tissues were obtained from the Human Protein Atlas[60] (https://proteinatlas.org), details regarding antibodies and patient numbers are included in the related figures.

Flow cytometry analysis

Organoids were released from BME and dissociated into single cells as described above. Post-dissociation, cells were incubated with primary antibody on ice for 30 min, followed by staining with DAPI or PI. Samples were analysed on a BD LSR Fortessa X20 equipped with four lasers (BD Bioscience) or a BD FACSMelody cell sorter equipped with three lasers (BD Bioscience). Cell sorting was performed on a BD FACS Influx cell sorter equipped with five lasers (BD Bioscience). BD FACS Diva software (v.8.0.1) and FlowJo (v.10.8.0) were used for data analysis and display. Sequential gating strategies for flow cytometry can be found in Supplementary Fig. 2.

Preparation of single-cell suspension from primary intestinal tissues: Human terminal ileum tissue was first dissected to remove the muscularis externa, following a previous protocol[61]. Regions containing human or mouse Peyer's patches, which could be clearly identified under dissection microscopy, were enriched, minced into small pieces (~1 mm^2), and digested in digestion buffer (adDMEM/F12 supplemented with 100 U ml^{-1} penicillin/streptomycin, 10 mM HEPES, 1× GlutaMAX, 1 mg ml^{-1} collagenase (Sigma-Aldrich, C9407), and 5 mM EDTA) for 30 min at 37 °C, with vigorous shaking every 5 min. The digested tissues were then filtered through a 100-µm cell strainer, washed twice with wash buffer (adDMEM/F12 supplemented with 100 U ml^{-1} penicillin/streptomycin, 10 mM HEPES, 1× GlutaMAX, and 10% FBS), and dissociated into single cells for flow cytometry analysis, similar to the procedure used for organoids, as described above.

Antibodies used in FACS analysis: mouse anti-human GP2-AF488 (MBL, D277-A48, clone 3G7-H9); rat anti-mouse GP2-AF488 (MBL, D278-A48, clone 2F11-C3); mouse anti-human ICAM2-biotin (Thermo Fisher, BMS109BT, clone CBR-IC2/2); mouse anti-human HLA-DP/DQ/DR-BV421 (BD horizon, 564244, clone Tu39); mouse anti-human HLA-DP/DQ/DR-FITC (BD Pharmingen, 562008, clone Tu39); mouse anti-human CD4-AF488 (Biolegend, 317420, clone OKT4); mouse anti-human EpCAM-APC (Biolegend, 369810, clone CO17-1A); rat anti-mouse MHC-II (I-A/I-E)-BV421 (Biolegend, 107631, clone M5/114.15.2); rat anti-mouse CD45-PE (Biolegend, 103106, clone 30-F11); rat anti-mouse EpCAM-APC (Thermo Fisher, 17-5791-80, clone G8.8); mouse anti-human CD69-PE (Biolegend, 310905, clone FN50). Antibodies were diluted 1:100.

Sample preparation and immunogold labelling for electron microscopy imaging

For TEM imaging, organoids were fixed with 1.5% glutaraldehyde in 0.1 M cacodylate buffer for 24 h at 4 °C. Following fixation, the samples were washed with 0.1 M cacodylate buffer and post-fixed with 1% osmium tetroxide in the same buffer containing 1.5% potassium ferricyanide for 1 h in the dark at 4 °C. The samples were then dehydrated in ethanol, infiltrated with Epon resin for 2 days, and subsequently embedded in the same resin. Polymerization of the resin was carried out at 60 °C for 48 h. Ultrathin sections (70 nm) were obtained using a Leica Ultracut UCT ultramicrotome (Leica Microsystems) and mounted on Formvar-coated copper grids. The ultrathin sections were stained with 2% uranyl acetate in water, followed by lead citrate. Images were captured using a Tecnai T12 electron microscope equipped with an Eagle 4kX4k CCD camera (Thermo Fisher Scientific).

To prepare ultrathin sections for immunolabelling, M cell organoids or normal intestinal organoids treated with or without IFNγ (48 h) were chemically fixed with 4% paraformaldehyde in 0.1 M phosphate buffer at 4 °C. After fixation, the organoids were washed with 0.1 M phosphate buffer, embedded in 12% gelatin, and infused in 2.3 M sucrose for 24 h. The mounted gelatin blocks were frozen in liquid nitrogen. Thin sections were prepared using a cryo ultramicrotome (Leica EM Ultracut UC6/FC6, Leica Microsystems). Ultrathin cryosections were collected with 2% methylcellulose in 2.3 M sucrose.

For immunogold labelling, cryosections were incubated on drops of PBS for 60 min at 37 °C, followed by incubation in 50 mM glycine in PBS for 10 min and 1% BSA in PBS for 15 min at room temperature. Sections were then incubated with mouse anti-human CD63 antibody (BD Biosciences, 556019, clone H5C6, diluted 1:20) or mouse anti-human MHC-II antibody (Thermo Fisher, MA1-25914, clone CR3/43,

diluted 1:20) diluted in 1% BSA in PBS for 60 min. After five washes with drops of 0.1% BSA in PBS, sections were incubated for 20 min with a bridging antibody, rabbit anti-mouse (DAKO, diluted 1:300). Following five additional washes with drops of 0.1% BSA in PBS, sections were incubated for 20 min with protein A-conjugated, 10 nm diameter colloidal gold particles (CMC Utrecht, diluted 1:50), diluted in 1% BSA in PBS. Sections were then fixed with 1% glutaraldehyde in PBS for 5 min, followed by washes with drops of PBS for 10 min, and two washes with distilled water. Grids were embedded in a thin layer of 1.8% methylcellulose (25 Ctp) containing 0.4% Uranyl acetate. A control for non-specific binding of the colloidal gold-conjugated antibody was included by omitting the primary antibody. Images were captured using the Tecnai T12 electron microscope equipped with the Eagle 4kX4k CCD camera.

Sample preparation and scRNA-seq analysis of M cell organoids

Differentiated M cell organoids were dissociated into single cells for FACS sorting as described above. Single DAPI$^-$ live cells were sorted using a BD FACS Influx cell sorter. Sorted individual single cells were collected in 384 well plates containing ERCC spike-ins (Agilent), reverse transcription primers (Promega) and dNTPs (Promega) as previously described[62]. A total of 768 cells (2 plates) were collected. scRNA-seq was conducted according to the SORT-seq method[63]. Sequencing libraries were prepared with TruSeq small RNA primers (Illumina) and sequenced on the Illumina NextSeq platform. Sequencing reads were aligned to the human GRCh38 genome to generate the gene expression matrix for subsequent analysis.

The scRNA-seq datasets were loaded into Seurat (v.3.1.4) objects in R Studio (v.3.6.3) for data integration, analysis and visualization[64], according to the standard pipeline. To create Seurat objects, data were filtered with nFeature_RNA values set to more than 1,000. In total of 375 cells fit this criterion. After creating the Seurat objects, data normalization was performed based on the LogNormalize method, with the scale. factor set to 10,000. Variable features were found by the vst method. Per plate, the two datasets were then anchored together with 2,000 integration features and 50 dimensions to find integration anchors before being clustered in accordance with the standard Seurat pipeline. Dimensional reduction was performed using the UMAP method based on the top 20 principal components. Cell clustering was based on the unsupervised shared-nearest neighbour (SNN) method with the resolution set to 0.7. A total of three cell clusters were identified and annotated, based on the well-known intestinal cell-type markers. Violin plots, heat maps and individual UMAP plots for the given genes were generated by the Seurat toolkit functions VlnPlot, DoHeatmap and DimPlot, respectively.

Re-analysis of primary human intestinal scRNA-seq datasets

Four published datasets were loaded into Seurat objects in R Studio for data integration and visualization. To create the Seurat objects, in GSE119969 (ref. 65) and GSE125970 (ref. 66) datasets, genes expressed in at least three cells and cells with nFeature_RNA > 200 were selected, in the GSE146799 (ref. 62) dataset, genes expressed in at least three cells and cells with nFeature_RNA > 1,000 were selected. We directly used the Seurat object created by Elmentaite et al.[17], but only selected cells from the adult and paediatric healthy donors in our analysis. To accelerate the speed of analysis, we removed the stem/TA cells and enterocytes from the Elmentaite et al. dataset. The other three datasets still contain sufficient numbers of these cells for analysis. Datasets were then anchored together with 2,000 integration features and 30 dimensions to find integration anchors before being clustered in accordance with the standard Seurat pipeline. Dimensional reduction was performed using UMAP method. Cell clustering was based on the unsupervised SNN method. After cell-type annotation, based on the well-known intestinal cell-type markers, we only used the cells with a clear cellular identity for further analysis and data display. Unsupervised sub-clustering of primary *SPIB*-expressing M cells was similarly done with the SNN method, by setting the resolution to 2, which identified six sub-clusters. The developmental stage of each sub-cluster was defined on the basis of the expression of well-known M cell markers: *GP2* for mature M cells, *ICAM2*, *TNFAIP2* and *CCL23* for immature M cells, and *SPIB* for early M cells.

Integration of human intestinal epithelial and immune cells: the Seurat object of primary intestinal myeloid cells, created by Elmentaite et al.[17], was included and integrated with the epithelial cell types derived from the Seurat object generated above, which includes enterocytes, Paneth cells, tuft cells, goblet cells and genuine M cells (excluding the Brunner's gland cells). MHC-II$^+$ enterocytes were derived from the IBD samples of Elmentaite et al. dataset. The datasets were anchored together based on 2,000 integration features and 30 dimensions. Dimensional reduction was performed using UMAP method and cell clustering was based on the unsupervised SNN method.

For transcriptomic comparisons of immature versus mature M cells or M cells versus MHC-II$^+$ enterocytes, the raw counts data were analysed using the DEseq2 (v.1.26.0) R package[67] with default settings. Normalized counts of MHC-II genes after DEseq2 analysis were shown in the Extended Data Fig. 7c. DEGs were defined by $|\log_2(\text{fold change})| \geq 2$ with P value ≤ 0.001. GO analysis was performed by uploading these DEGs into the Enrichr software[68] to identify the most relevant cell types.

Re-analysis of scRNA-seq datasets of mouse intestinal tissue- or organoid-derived M cells

Sequencing data[29] of mouse intestinal organoids cultured with or without RANKL was retrieved from the GEO database (GSE92332). Analysis was performed in Python (v.3.11.9) using the Scanpy library and the recipe based on Wu et al.[69]. In brief, cells with more than 5% mitochondrial genes were filtered out, and counts per cell were normalized and $\log_{10}$-transformed. Dimensional reduction was performed by finding the 2,000 most highly expressed genes (excluding mitochondrial and ribosomal), scaling and principal components analysis (50 components) and computing of the neighbourhood graph (k-nearest neighbours (KNN) = 200).

Sequencing data of primary mouse intestinal cell types were also retrieved from the GEO database (GSE92332). Raw counts data of M cells and distal enterocytes (cell-type annotation same as the original study) were subjected to DEseq2 analysis with default settings. Normalized counts of MHC-II genes after DEseq2 analysis were shown in the Extended Data Fig. 7c. GO analysis was performed using the mouse M cell marker genes (revealed by the original study) and the Enrichr software to identify the most relevant functional pathways.

T cell binding assay in co-culture

CD4$^+$ T cells were activated to induce LFA-1 expression by Dynabeads Human T-Activator CD3/CD28 for T Cell Expansion and Activation (Thermo Fisher, 11131D). M cell organoids were released from BME and co-cultured with activated CD4$^+$ T cells for 6 h in suspension culture to facilitate T cell binding. After incubation, the organoids with bound T cells were gently collected into a 15-ml tube containing 13 ml of culture medium. Organoids were allowed to spontaneously settle by gravity for 3–4 min. The supernatant containing unbound T cells was then removed. Organoids were then washed twice using the same method to thoroughly remove the remaining unbound T cells, collected by centrifugation, and dissociated into single cells followed by flow cytometry analysis. The number of CD4$^+$ T cells that still bind to organoids was normalized against the number of EpCAM$^+$ epithelial cells. To inhibit T cell binding, *ICAM2* knockout M cell organoids were used, and an ICAM1 neutralizing antibody[70] (10 μg ml^{-1}, Thermo Fisher, 15-0549-82) was further added 1 h prior to the T cells.

Phagocytosis of bacteria particles in 2D cultured M cells

FACS-sorted M cells were seeded on glass-bottom 96-well plates coated with Invasin[71] to facilitate cell attachment. After overnight culture,

fluorescent bacteria particles were prepared and added according to the manufacturer's protocol (Thermo Fisher, P35361), followed by live imaging. For live imaging, plates were staged on the Leica SP8 confocal detection system fitted on a Leica DMi8 microscope (equipped with a CO_2 and temperature control system) to capture time-series images every 5 min for 2 h. Images were analysed and movie was generated by the IMARIS software (v.9.3). The phagocytosis inhibitor cytochalasin B (10 μM, Sigma-Aldrich, C6762) was added 3 h prior to the addition of bacteria particles.

Preparation of 33-mer peptides and wheat-derived gliadin protein

To prepare pepsin/trypsin-treated gliadin protein, 10 g of wheat-derived gliadin (Sigma-Aldrich, G3375) was dissolved in 100 ml of 0.2 N hydrochloric acid, followed by pepsin treatment (Sigma-Aldrich, P6887, 2 mg ml^{-1}) for 2 h at 37 °C, with stirring. pH of the mixture was adjusted to 7.4 using 2 M sodium hydroxide. Subsequent trypsin treatment (Sigma-Aldrich, T1416) was performed at 37 °C for 4 h, with vigorous stirring. The mixture was then heated at 100 °C for 30 min to stop enzyme activity, and freeze-dried into powder. Further TGM2 (tissue transglutaminase) treatment was performed by incubating 1.08 ml dissolved powder (prepared as 1.11 mg ml^{-1} in PBS) with 120 μl TGM2 enzyme (Sigma-Aldrich, T5398, prepared as 1 mg ml^{-1} in PBS containing 1 mM $CaCl_2$) for 2 h at 37 °C. The 33-mer peptides were synthesized by GenScript, with the sequence LQLQPF(PQPELPY)3PQPQPF and LQLQPF(PQPQLPY)3PQPQPF.

Reporter T cell lines with TCR overexpression

The human Jurkat T cell line derivative J76 reporter cell line (J76TPR[72]), provided M. H. M. Heemskerk, was utilized in this study. The HLA-DQ2.5-glia-α2 specific TCR sequence S16 (TCRα-P2A-TCRβ) was cloned into a plasmid containing the PiggyBac Transposon system. J76TPR cells, which lack endogenous TCRα and TCRβ chains, were transfected with the S16 TCR and transposase plasmids through electroporation. The surface expression of the S16 TCR was evaluated by flow cytometry with the staining of an APC-conjugated anti-human TCR α/β antibody (Biolegend, 306718, clone IP26). Cells expressing the S16 TCR were FACS-sorted and cultured in IMDM (Iscove's Modified Dulbecco's Medium, Gibco, 12440061) supplemented with 10% heat-inactivated FBS, 100 μg ml^{-1} streptomycin, and 100 U ml^{-1} penicillin. The expression of the S16 TCR was routinely checked by flow cytometry every two weeks for use in subsequent experiments.

The human Jurkat T cell line derivative JRT3 cell line, with endogenous TCRα and TCRβ chains knockout, expressing NFAT-RE-Luc2 and HLA-DQ2.5-glia-α2 specific TCR D2, was provided by Chugai Pharmaceutical. These cells were cultured in RPMI1640 (Roswell Park Memorial Institute 1640 medium, Gibco, 11875093) supplemented with 10% heat-inactivated FBS, 100 μg ml^{-1} streptomycin, 100 U ml^{-1} penicillin, 1 x MEM non-essential amino acids, 1 mM sodium pyruvate, 0.2 mg ml^{-1} hygromycin and 100 μg ml^{-1} zeocin. Both cell lines were validated on the basis of gliadin-specific T cell activation, as indicated by the induced reporter gene expression, and were assessed and scored negative for mycoplasma contamination.

CeD PBMC isolation

Peripheral blood collected in EDTA tubes was processed for mononuclear cell isolation using BD Vacutainer Mononuclear Cell Preparation Tubes (CPT, BD Biosciences). A volume of 8 ml of whole blood was transferred into a CPT tube, followed by gentle inversion ten times to ensure proper mixing with the separation medium. Immediately prior to centrifugation, the tube was inverted an additional three times to homogenize the contents. Samples were centrifuged at room temperature for 15 min at a relative centrifugal force (RCF) of 1,500–1,800*g*. Following centrifugation, approximately 50% of the plasma layer was carefully aspirated without disturbing the underlying mononuclear cell layer, which appeared as a diffuse, cloudy interface. The entire cell layer was then collected using a disposable plastic Pasteur pipette and transferred into a sterile 15 ml conical tube. To wash the cells, 10 ml of PBS was added and the tube was gently inverted to mix. The suspension was centrifuged for 10 min at 300*g* at room temperature. During this step, a freezing medium was prepared, consisting of 80% heat FBS (Thermo Fisher) and 20% DMSO (Sigma-Aldrich). After centrifugation, the supernatant was discarded. The cells were resuspended in 0.5 ml of RPMI1640 medium (Thermo Fisher) and transferred into a cryovial containing 0.5 ml of freezing medium, with gentle mixing to ensure homogeneity. The cryovials were then placed in a freezing container and stored at −80 °C for controlled-rate freezing.

Co-culture of reporter T cells with organoids and analysis of T cell activation

Organoids cultured in M cell medium or OCHIO medium (with or without IFNγ stimulation for 48 h) for 6–7 days were washed twice with wash medium (adDMEM/F12 supplemented with 100 U ml^{-1} penicillin/streptomycin, 10 mM HEPES and 1× Glutamax) and broken into small pieces by mechanical shearing to ensure better antigen uptake. 10 μg ml^{-1} of 33-mer peptides or 20 μg ml^{-1} of gliadin proteins were added to the organoids for 5 h prior to co-culture. J76TPR cells expressing S16 TCR or JRT3 cells expressing D2 TCR were counted and co-cultured with antigen pre-treated organoids at a 1:1 ratio. The organoid and T cell co-cultures were maintained overnight in a co-culture medium consisting of 48.75% OCHIO medium, 48.75% T cell medium, and 2.5% BME. T cell activation in J76TPR was assessed by flow cytometry. Cells were stained with the APC-conjugated anti-human TCR α/β antibody. Then the eGFP fluorescence from the NFAT-RE-eGFP reporter construct in J76TPR cell line was analysed, as an indicator of T cell activation. T cell activation in JRT3 cells was assessed by measuring the luciferase activity using the Steady-Glo Luciferase Assay System (Promega, E2510) according to the manufacturer's protocol. The luminescence intensity of each well was recorded for 1,000 ms using the Spark multimode microplate reader (TECAN Life Sciences). The induction of luciferase activity was quantified by calculating the ratio of the difference between the luminescence counts per second (cps) of the target wells and the average luminescence cps of the cell-free wells to the difference between the average luminescence cps of the T cell-only wells and the average luminescence cps of the cell-free wells.

Co-culture of primary human T cells with M cells and analysis of T cell activation

Organoids cultured in M cell medium or OCHIO medium (with or without IFNγ stimulation for 48 h) for 6–7 days were collected as a single-cell suspension as described above. Cells were then stained with antibodies and FACS-sorted into MHC-II^+ and MHC-II^- populations for the following co-culture assays. All experiments were performed in flat bottom 96-well plates (Greiner, 655180) pre-coated overnight at 4 °C with 1% BME in PBS.

For antigen-dependent activation of autologous T cells, 20,000 FACS-sorted MHC-II^+ and MHC-II^- organoid cells were plated and incubated overnight with a human MHC-II-restricted peptide pool (JPT Peptide Technologies, PM-CEFT-MHC-II-1; 5 μg ml^{-1}). The following day, 100,000 naive $CD4^+$ T cells isolated from autologous PBMCs using MojoSort Human naive $CD4^+$ T cell Isolation Kit (Biolegend, 480041) were added to the co-culture. After 24 h, T cell activation was analysed by flow cytometry following staining with DAPI, anti-CD4-AF488 (Biolegend, 317420), and anti-CD69-PE (Biolegend, 310905) FACS antibodies. The setting of the $CD69^+$ gate was based on the negative controls.

For antigen-independent stimulation, FACS-sorted MHC-II^+ and MHC-II^- cells were plated (20,000 per well) and co-cultured 3 h later with 100,000 naive $CD4^+$ T cells from unrelated healthy donors. CytoStim (Miltenyi Biotec, 130-092-173) was added following the

manufacturer's protocol. After 24 h, CD69 upregulation was assessed as described above. For proliferation analysis, naive $CD4^+$ T cells were pre-labelled with Cell Proliferation Dye eFluor 670 (Thermo Fisher, 65-0840-85) and analysed by flow cytometry after five days, following staining with anti-CD4-AF488 antibody.

To assess gluten-specific responses, MHC-II^+ and MHC-II^- cells of organoids derived from HLA-DQ2.5 donor were FACS-sorted and plated as described above. The 33-mer gliadin peptides (10 μg ml^{-1}) were added for overnight incubation. Total $CD4^+$ T cells were isolated from PBMCs of patients with CeD with the HLA-DQ2.5 haplotype, using the MojoSort Human $CD4^+$ T cell Isolation Kit (Biolegend, 480009), and co-cultured at 100,000 cells per well. T cell activation was evaluated by flow cytometry following DAPI, CD4 and CD69 staining.

EdU labelling assay

Cultured organoids were incubated with EdU (1 mg ml^{-1}) for 2 h, followed by 1 h fixation with 4% formaldehyde solution at room temperature. EdU colour development was performed following manufacturer's protocol (Thermo Fisher, C10640).

TGM2 ELISA

Cell lysates and culture media from M cell organoids were analysed by ELISA following the manufacturer's protocol (Thermo Fisher, EH462RB). To prepare the samples, M cell organoids were collected and washed three times with PBS to thoroughly remove remaining BME, then lysed with lysis buffer (Thermo Fisher, 87787). Culture medium was pre-concentrated tenfold using Protein Concentrators (Thermo Fisher).

Bulk RNA sequencing of M cell organoids

For each M cell subpopulation, 2,000 $DAPI^-$ live single cells (from one biological replicate) were FACS-sorted into the TRIzol reagent (Thermo Fisher, 15596026). Library preparation and sequencing were performed by Single Cell Discovery following the standard protocol. Sequencing reads were aligned to the human GRCh38 genome. Raw counts data was subjected to DEseq2 R package[67] and analysed with default settings. DEGs were defined by $|\log_2(\text{fold change})| \geq 1$ with P value ≤ 0.01. GO analysis was performed by uploading the DEGs into the Enrichr web software. GSEA was based on clusterProfiler (v.3.14.3) R package[73]. $\log_2$ (fold change) was calculated between the mature M cells and enterocytes. The KEGG gene sets (v.7.4) and all GO gene sets (v.7.4) were used as the reference.

RNA extraction and qPCR analysis

Following the manufacturer's protocol, FACS-sorted cells were subjected to RNA isolation using a NucleoSpin RNA kit (Macherey-Nagel, 740955.50). Reverse transcription reactions were performed using GoScript reverse transcriptase kit (Promega, A5000). cDNA was subjected to qPCR analysis using iQ SYBR Green Supermix (Bio-Rad, 1708887) on a CFX Connect Real-Time PCR machine (Bio-Rad). For gene expression analysis, qPCR was performed with gene-specific qPCR primers. The Ct value of each gene was normalized to the housekeeping gene GAPDH (as the ΔC_t), and fold change between experimental groups was calculated with the $2^{-\Delta\Delta Ct}$ method. All qPCR primers used in this study are listed in Supplementary Table 2.

Quantification and statistics analysis

Data were presented as mean ± s.e.m. Two-tailed Student's t-test was used when two experimental groups were compared. One-way ANOVA was used when multiple experimental groups were compared. All P values were calculated and all the graphs were generated using Graphpad PRISM (v.7.04). The statistical details for each experiment can be found in the figure legends. In volcano plots shown in (Extended Data Figs. 2c, 3c,e and 6d), DEseq2 used negative-binomial generalized linear models (NB-GLM) and tested coefficients (per gene) with two-sided Wald test to produce P values. In volcano plots shown in (Figs. 2i and 3c and Extended Data Figs. 6f and 7d), P values were computed from one-sided Fisher's exact test, which is a proportion test that assumes a binomial distribution and independence for probability of any gene belonging to any test.

Reporting summary

Further information on research design is available in the Nature Portfolio Reporting Summary linked to this article.

Data availability

The organoid scRNA-seq and bulk RNA-seq datasets generated in this study have been deposited and are publicly available in the Gene Expression Omnibus (GEO, www.ncbi.nlm.nih.gov/geo/) under accession codes GSE275771 and GSE275772. We re-analysed the following publicly available scRNA-seq datasets: GSE119969 (GSM3389578, GSM3389579 and GSM3389580;), GSE125970 (raw_UMIcounts.txt.gz;), GSE146799 (EEC_atlas_raw.csv.gz;), GSE92332 (FAE_UMIcounts.txt.gz and Org_RANKL_UMIcounts.txt.gz;), and Space-Time Gut Cell Atlas (datasets for epithelium and myeloid cells; https://www.gutcellatlas.org). Source data are provided with this paper.

Code availability

No custom code was generated in this study. scRNA-seq and bulk RNA-seq analysis were performed using Seurat[64] and DESeq2 (ref. 67) R packages, respectively. Details have been described in the Methods and scripts used to produce all related plots in the figures are available in the source data.

51. Sato, T. et al. Single Lgr5 stem cells build crypt–villus structures in vitro without a mesenchymal niche. *Nature* **459**, 262–265 (2009).
52. Wang, D. et al. Interferon-responsive intestinal BEST4/$CA7^+$ cells are targets of bacterial diarrheal toxins. *Cell Stem Cell* **32**, 598–612.e5 (2025).
53. Pleguezuelos-Manzano, C. et al. Establishment and culture of human intestinal organoids derived from adult stem cells. *Curr. Protoc. Immunol.* **130**, e106 (2020).
54. Ran, F. A. et al. Genome engineering using the CRISPR-Cas9 system. *Nat. Protoc.* **8**, 2281–2308 (2013).
55. Artegiani, B. et al. Fast and efficient generation of knock-in human organoids using homology-independent CRISPR–Cas9 precision genome editing. *Nat. Cell Biol.* **22**, 321–331 (2020).
56. Hendriks, D., Artegiani, B., Hu, H., Chuva de Sousa Lopes, S. & Clevers, H. Establishment of human fetal hepatocyte organoids and CRISPR–Cas9-based gene knockin and knockout in organoid cultures from human liver. *Nat. Protoc.* **16**, 182–217 (2020).
57. Komor, A. C., Kim, Y. B., Packer, M. S., Zuris, J. A. & Liu, D. R. Programmable editing of a target base in genomic DNA without double-stranded DNA cleavage. *Nature* **533**, 420–424 (2016).
58. Andersson-Rolf, A. et al. One-step generation of conditional and reversible gene knockouts. *Nat. Methods* **14**, 287–289 (2017).
59. Cong, L. et al. Multiplex genome engineering using CRISPR/Cas systems. *Science* **339**, 819–823 (2013).
60. Uhlén, M. et al. Tissue-based map of the human proteome. *Science* **347**, 1260419 (2015).
61. Jørgensen, P. B. et al. Identification, isolation and analysis of human gut-associated lymphoid tissues. *Nat. Protoc.* **16**, 2051–2067 (2021).
62. Beumer, J. et al. High-resolution mRNA and secretome atlas of human enteroendocrine cells. *Cell* **181**, 1291–1306.e19 (2020).
63. Muraro, M. J. et al. A single-cell transcriptome atlas of the human pancreas. *Cell Syst.* **3**, 385–394.e3 (2016).
64. Butler, A., Hoffman, P., Smibert, P., Papalexi, E. & Satija, R. Integrating single-cell transcriptomic data across different conditions, technologies, and species. *Nat. Biotechnol.* **36**, 411–420 (2018).
65. Fujii, M. et al. Human intestinal organoids maintain self-renewal capacity and cellular diversity in niche-inspired culture condition. *Cell Stem Cell* **23**, 787–793.e6 (2018).
66. Wang, Y. et al. Single-cell transcriptome analysis reveals differential nutrient absorption functions in human intestine. *J. Exp. Med.* **217**, e20191130 (2020).
67. Love, M. I., Huber, W. & Anders, S. Moderated estimation of fold change and dispersion for RNA-seq data with DESeq2. *Genome Biol.* **15**, 550 (2014).
68. Xie, Z. et al. Gene set knowledge discovery with Enrichr. *Curr. Protoc.* **1**, e90 (2021).
69. Wu, X. S. et al. OCA-T1 and OCA-T2 are coactivators of POU2F3 in the tuft cell lineage. *Nature* **607**, 169–175 (2022).
70. Lieberman, P. M. et al. Pomalidomide restores immune recognition of primary effusion lymphoma through upregulation of ICAM-1 and B7-2. *PLoS Pathog.* **17**, e1009091 (2021).
71. Wijnakker, J. J. A. P. M. et al. Integrin-activating *Yersinia* protein Invasin sustains long-term expansion of primary epithelial cells as 2D organoid sheets. *Proc. Natl Acad. Sci. USA* **122**, e2420595121 (2025).
72. Rosskopf, S. et al. A Jurkat 76 based triple parameter reporter system to evaluate TCR functions and adoptive T cell strategies. *Oncotarget* **9**, 17608–17619 (2018).

73. Yu, G., Wang, L. G., Han, Y. & He, Q. Y. clusterProfiler: an R package for comparing biological themes among gene clusters. *OMICS* **16**, 284–287 (2012).

Acknowledgements We thank R. van der Linden and A. Pfauth for cell sorting; Single Cell Discovery for technical support in scRNA-seq and bulk RNA-seq experiments; A. K. Balwierz for assistance in scRNA-seq experiments; M. H. M. Heemskerk for sharing the J76 reporter cell line (J76TPR). This work is supported by: the Netherlands Organ-on-Chip Initiative, an NWO Gravitation project (nr. 024.003.001) funded by the Ministry of Education, Culture and Science of the government of the Netherlands (to H.C.); the project Organoids in Time with project no. 2019.085 of the research programme NWO Investment Large, financed by the Dutch Research Council (to H.C., J.S.v.Z. and S.J.T.); The Oncode Institute (partly financed by the Dutch Cancer Society).

Author contributions D.W. and S.L. conceptualized the project, designed and performed experiments, interpreted the results and wrote the manuscript. W.J.v.d.W., C.L.-I. and P.J.P. performed electron microscopy imaging and interpreted the results. Y.O., Y.T.-I. and A.M. generated the DONQ52 antibody and provided the JRT3 reporter T cell line. W.K.S., J.S.v.Z. and S.J.T. performed scRNA-seq analysis of previously published mouse M cell organoids. T.D. established several organoid lines used in this study. G.J.F.v.S. assisted in scRNA-seq analysis of human datasets. A.P. and N.S. provided the human terminal ileum tissues. G.B.C.G.-d.J., S.W. and I.H.J. prepared and provided the CeD PBMCs. J.H.v.E. and H.C. conceptualized and supervised the project and wrote the manuscript.

Competing interests H.C. was the head of Pharma Research and Early Development at Roche, Basel and holds several patents related to organoids technology. His full disclosure can be found at https://www.uu.nl/staff/JCClevers/AncillaryActivities. Y.O., Y.T.-I. and A.M. are employees of Chugai Pharmaceutical and inventors on patents (WO 2022/059766) related to DONQ52, of which all rights have been assigned to the company.

Additional information

Supplementary information The online version contains supplementary material available at https://doi.org/10.1038/s41586-025-09829-8.

Correspondence and requests for materials should be addressed to Hans Clevers.

Peer review information *Nature* thanks Dan Littman, Toshiro Sato, Ludvig Sollid and the other, anonymous, reviewer(s) for their contribution to the peer review of this work. Peer review reports are available.

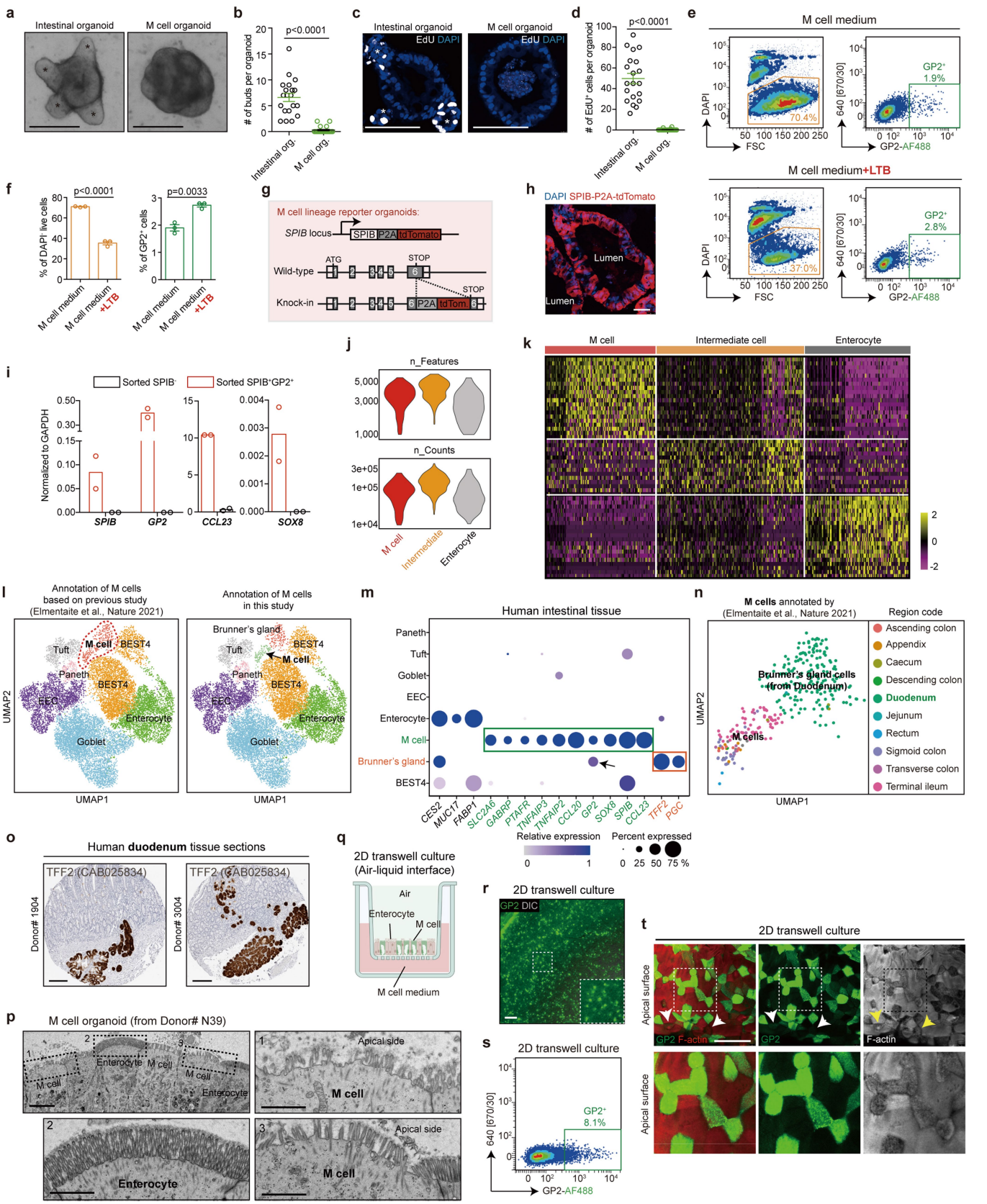

Extended Data Fig. 1 | See next page for caption.

Extended Data Fig. 1 | Generation and characterization of human M cell organoids. (**a,b**) Representative bright-filed images of cultured M cell organoids versus normal intestinal organoids (**a**). The number of buds per organoid is quantified in (**b**). n = 20 organoids for each group. Each dot represents one organoid. Three independent experiments are performed on two donors with similar results. Data are presented as mean values +/− SEM. P-values are derived from two-tailed t-test. Scale bars, 100 µm. (**c,d**) Representative confocal images showing the EdU^+ proliferating cells in cultured M cell organoids versus normal intestinal organoids (**c**). The number of EdU^+ cells per organoid is quantified in (**d**). n = 20 organoids for each group. Each dot represents one organoid. Three independent experiments are performed on two donors with similar results. Data are presented as mean values +/− SEM. P-values are derived from two-tailed t-test. Scale bars, 100 µm. (**e,f**) Representative flow cytometry analysis (**e**) and quantification of $DAPI^-$ live cells or $GP2^+$ M cells (**f**) in cultured M cell organoids (Ctrl) or adding LTB during M cell differentiation. n = 3 independent wells on one donor. Each dot represents one well. Data are presented as mean values +/− SEM. P-values are derived from two-tailed t-test. (**g**) Illustration of the knock-in reporter organoids containing a *P2A-tdTomato* cassette inserted at the C-terminus, before the stop codon, of the *SPIB* gene. (**h**) Representative confocal image of *SPIB-P2A-tdTomato* reporter organoids cultured in M cell medium. M cells are marked by tdTomato fluorescence (red). Three independent experiments are performed on one donor with similar results. Scale bar, 50 µm. (**i**) qPCR analysis of the expression levels of a set of M cell markers in FACS-sorted $SPIB^-$ and $SPIB^+GP2^+$ cells. n = 2 technical replicates are shown. Data are presented as mean values. Results are representative of two independent experiments on one donor. (**j**) Quality control of scRNA-seq dataset derived from human M cell organoids. Numbers of features (top) and counts (bottom) per cell are shown across different cell types. n = 375 single cells. (**k**) Heatmap of cell type-enriched genes in scRNA-seq dataset of human M cell organoids. Each column represents a single cell and each row represents one marker gene. The colors, ranging from purple to yellow, indicate low to high relative gene expression levels. (**l**) scRNA-seq analysis of primary human intestinal cells. Cell clusters are visualized in UMAP plots and colored by different cell types. n = 15,543 single cells. Annotations of M cells based on a previous study (left) and in this study (right) are shown, respectively. (**m**) Dot plot showing the expression levels of a set of cell type-specific markers across primary intestinal cell types. n = 15,543 single cells. Dot color relates to normalized mean expression values and dot size to fraction of expressing cells. (**n**) UMAP plot showing the primary M cells colored by region code. Annotations of M cells are based on a previous study. n = 301 single cells. (**o**) IHC staining of TFF2 antibody on human duodenum tissue sections. Positive staining signals are detected in Brunner's gland cells. Images are derived from the Human Protein Atlas (proteinatlas.org). Similar results are observed in tissues from two donors. Scale bars, 100 µm. (**p**) Representative transmission electron microscopy images of M cell organoids. M cells are identified by having fewer apical microvilli compared to the neighboring enterocytes. M cell organoids from two donors are tested with similar results (see also Fig. 1h). Scale bars, 5 µm in low-magnification image and 2 µm in high-magnification images. (**q**) Schematic of air-liquid interface (ALI) system for M cell differentiation in monolayer culture. Images were created in BioRender. van Es, J. (2025) https://BioRender.com/xh7haut. (**r**) Representative images showing the ALI monolayer culture containing $GP2^+$ M cells. Three independent experiments are performed on two donors with similar results. Scale bar, 50 µm. (**s**) Representative flow cytometry analysis of $GP2^+$ M cells in ALI monolayer culture. Three independent experiments are performed on two donors with similar results. (**t**) Representative confocal images showing the $GP2^+$ M cells with fewer apical microvilli. M cells are identified by IF staining of GP2 antibody (green). Microvilli structures are detected by staining of F-actin using Phalloidin (red/white). Two $GP2^-$ cells also exhibit fewer microvilli (arrows). Three independent experiments are performed on two donors with similar results. Scale bar, 20 µm.

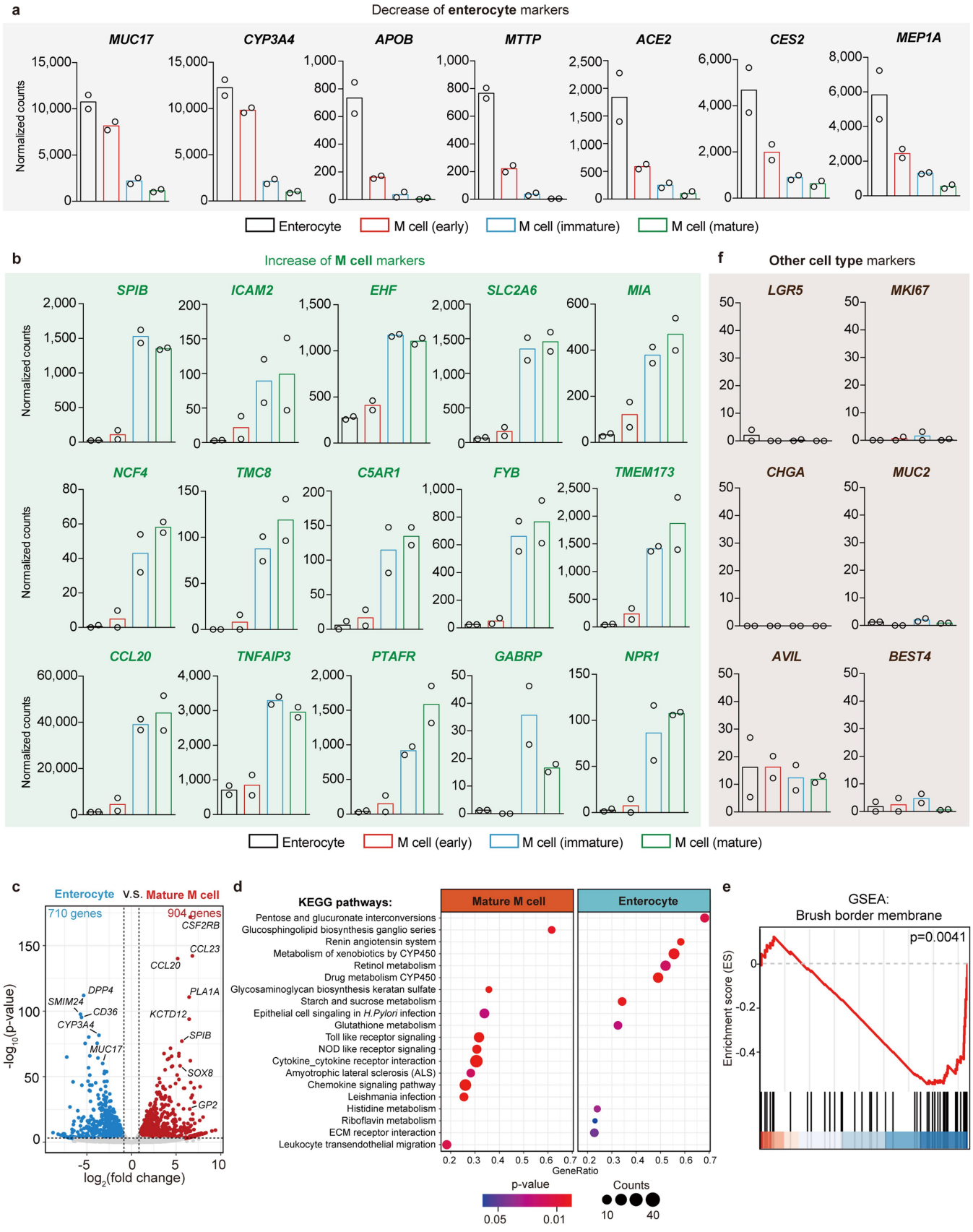

Extended Data Fig. 2 | See next page for caption.

Extended Data Fig. 2 | Transcriptomic changes during M cell maturation. (**a,b**) Expression levels (normalized counts) of a set of enterocyte (**a**) and M cell (**b**) specific markers across the indicated cell populations. n = 2 biological replicates. Data are presented as mean values. (**c**) Volcano plot showing the DEGs between enterocytes and mature M cells. P-values are derived from two-sided Wald test. (**d,e**) GSEA analysis showing the KEGG pathways enriched in enterocytes versus mature M cells and confirming decreased expression of brush border genes in mature M cells compared to enterocytes. GSEA uses a weighted Kolmogorov-Smirnov-style enrichment score (ES) with permutation-derived nominal p-values that are assessed one-sided for each enrichment direction. (**f**) Expression levels (normalized counts) of a set of cell type-specific markers across the indicated cell populations. n = 2 biological replicates. Data are presented as mean values.

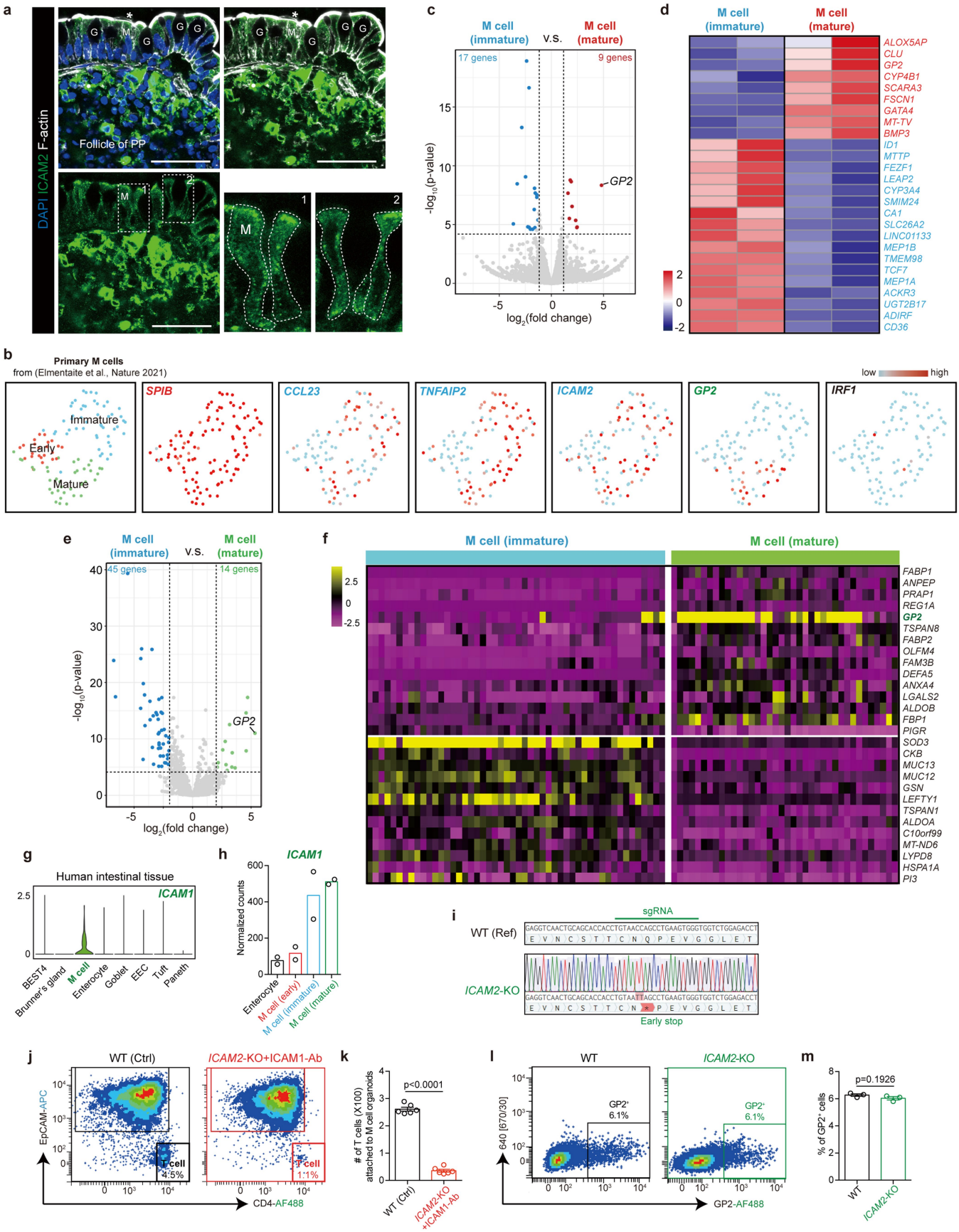

Extended Data Fig. 3 | See next page for caption.

Extended Data Fig. 3 | ICAM2 is a functional marker for immature and mature M cells. (**a**) Representative confocal images showing the ICAM2$^+$ M cells, identified by ICAM2 antibody staining (green), in human PP epithelium. Microvilli structures are detected by staining of F-actin using Phalloidin (white). One ICAM2$^+$ M cell with fewer microvilli (mature M cell) is marked by asterisk. M, mature M cell. G, goblet cell. Similar results are observed on PP tissues from two donors. Scale bars, 50 µm. (**b**) scRNA-seq analysis of primary M cells. The SPIB-expressing M cells are sub-clusters and visualized in UMAP plots, colored by different differentiation stages. n = 111 single cells. Expression levels and distributions of M cell markers and *IRF1* are shown in UMAP plots. (**c,d**) Volcano plot (**c**) and heatmap (**d**) showing the DEGs between immature and mature M cells derived from organoids. P-values are derived from two-sided Wald test in (**c**). (**e,f**) Volcano plot (**e**) and heatmap (**f**) showing the DEGs between immature and mature primary M cells. P-values are derived from two-sided Wald test in (**e**). (**g**) Violin plot showing the expression levels of *ICAM1* across multiple human intestinal cell types from tissue-derived scRNA-seq datasets containing 15,543 cells. (**h**) Expression levels (normalized counts) of *ICAM1* across the indicated cell populations. n = 2 biological replicates. Data are presented as mean values. (**i**) Validation of *ICAM2* KO by targeted genotyping. (**j,k**) Representative flow cytometry analysis (**j**) and quantification of CD4$^+$ T cells (**k**) that attached to M cell organoids in co-culture assays. An ICAM1 neutralizing antibody is added into the *ICAM2*-KO organoids. n = 6 independent co-culture wells on one donor. Each dot represents one well. Data are presented as mean values +/− SEM. P-values are derived from two-tailed t-test. (**l,m**) Representative flow cytometry analysis (**l**) and quantification of GP2$^+$ M cell percentage (**m**) in WT or *ICAM2*-KO organoids cultured in M cell medium. n = 3 independent wells on one donor. Each dot represents one well. Data are presented as mean values +/− SEM. P-values are derived from Two-tailed t-test.

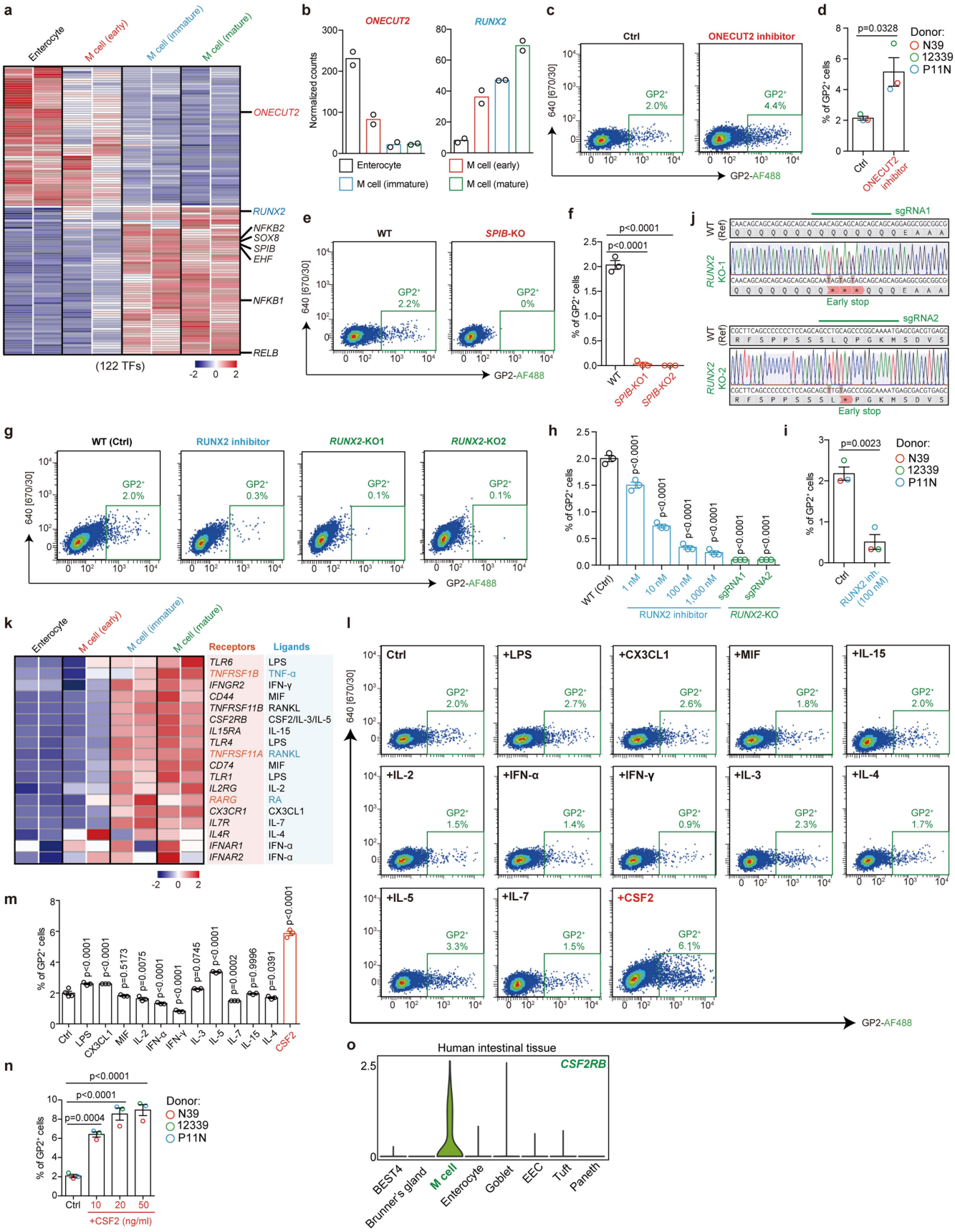

Extended Data Fig. 4 | See next page for caption.

Extended Data Fig. 4 | RUNX2 and CSF2 regulate human M cell differentiation. (**a**) Heatmap showing the expression patterns of differentially expressed TFs during M cell differentiation. n = 2 biological replicates. (**b**) Expression levels (normalized counts) of *ONECUT2* and *RUNX2* across the indicated cell populations. n = 2 biological replicates. Data are presented as mean values. (**c,d**) Representative flow cytometry analysis (**c**) and quantification of $GP2^+$ M cell percentage (**d**) in cultured M cell organoids (Ctrl) or adding ONECUT2 inhibitor during M cell differentiation. Three different donors are tested and shown in (**d**). Each dot represents the mean value derived from three independent wells. Data are presented as mean values +/− SEM. P-values are derived from two-tailed t-test. (**e,f**) Representative flow cytometry analysis (**e**) and quantification of $GP2^+$ M cell percentage (**f**) in WT or *SPIB*-KO organoids cultured in M cell medium. n = 2 *SPIB*-KO clonal organoid lines derived from one donor are tested. In each group, n = 3 independent wells. Each dot represents one well. Data are presented as mean values +/− SEM. P-values are derived from one-way ANOVA with Dunnett's test. (**g,h**) Representative flow cytometry analysis (**g**) and quantification of $GP2^+$ M cell percentage (**h**) in WT or *RUNX2*-KO organoids cultured in M cell medium or adding RUNX2 inhibitor during M cell differentiation. n = 2 *RUNX2*-KO clonal organoid lines derived from one donor are tested. In each group, n = 3 independent wells. Each dot represents one well. Data are presented as mean values +/− SEM. P-values are derived from one-way ANOVA with Dunnett's test. (**i**) Quantification of $GP2^+$ M cell percentage in cultured M cell organoids (Ctrl) or adding RUNX2 inhibitor during M cell differentiation. Three different donors are tested and shown. Each dot represents the mean value derived from three independent wells. Data are presented as mean values +/− SEM. P-values are derived from two-tailed t-test. (**j**) Validation of *RUNX2* KO by targeted genotyping. (**k**) Heatmap showing the expression patterns of differentially expressed receptors during M cell differentiation. Ligands for these receptors are indicated. n = 2 biological replicates. (**l,m**) Representative flow cytometry analysis (**l**) and quantification of $GP2^+$ M cell percentage (**m**) in cultured M cell organoids (Ctrl) or adding different immune factors during M cell differentiation. For each tested factor, n = 3 or 4 independent wells on one donor. Each dot represents one well. Data are presented as mean values +/− SEM. P values are derived from one-way ANOVA with Dunnett's test. (**n**) Quantification of $GP2^+$ M cell percentage in cultured M cell organoids (Ctrl) or adding CSF2 during M cell differentiation. Three different donors are tested and shown. Each dot represents the mean value derived from three independent wells. Data are presented as mean values +/− SEM. P-values are derived from one-way ANOVA with Dunnett's test. (**o**) Violin plot showing the expression levels of *CSF2RB* across multiple human intestinal cell types from tissue-derived scRNA-seq datasets containing 15,543 cells.

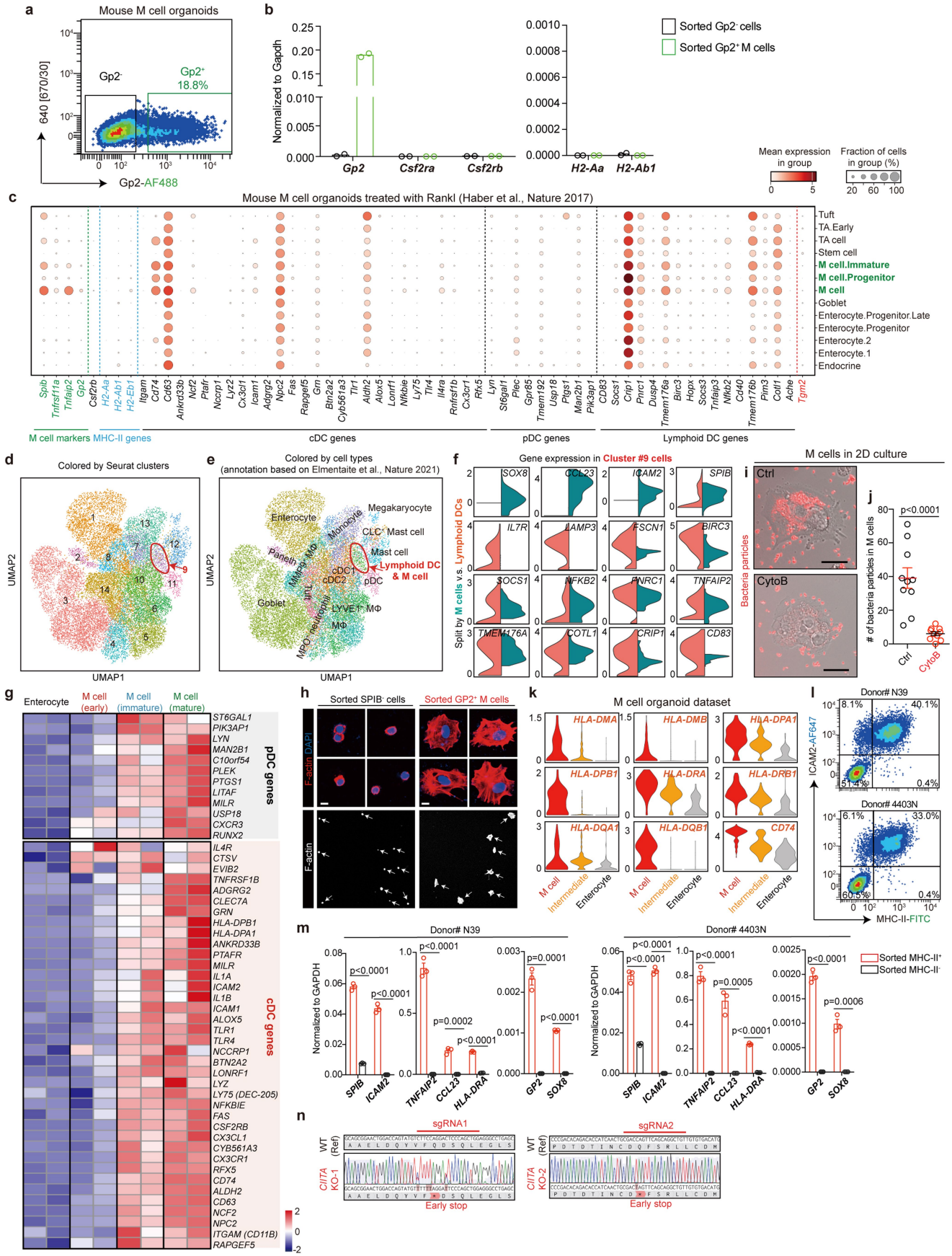

Extended Data Fig. 5 | See next page for caption.

Extended Data Fig. 5 | Analysis of DC-related genes in murine and human M cells. (**a**) Representative flow cytometry analysis of $Gp2^+$ M cells in murine M cell organoids. Three independent experiments are performed with similar results. (**b**) qPCR analysis of the expression levels of Gp2, Csf2 receptors, and MHC-II genes in FACS-isolated $Gp2^-$ and $Gp2^+$ cells from murine M cell organoids. n = 2 technical replicates are shown. Data are presented as mean values. Results are representative of two independent experiments. (**c**) Dot plot showing the expression levels of M cell markers, *Csf2rb*, *Tgm2*, MHC-II genes, and a set of DC markers across multiple mouse intestinal cell types derived from the organoids. n = 5,091 single cells. Dot color relates to normalized mean expression values and dot size to fraction of expressing cells. (**d,e**) scRNA-seq analysis of primary human intestinal cells. Multiple epithelial and immune cell types are integrated unbiasedly (See also Methods). Cell clusters are visualized in UMAP plots and colored by unsupervised clustering (**d**) or annotated cell types (**e**). n = 20,210 single cells. M cells and lymphoid DCs are clustered together in cluster #9, as indicated by the red circles. (**f**) Violin plots showing the expression levels of M cell and lymphoid DC markers in cells derived from cluster #9. n = 255 single cells. Cluster #9 cells are split into M cells and lymphoid DCs for comparisons. (**g**) Heatmap showing the expression patterns of a set of pDC and cDC markers during M cell differentiation. n = 2 biological replicates. (**h**) Representative confocal images showing the morphology of 2D-cultured non-M ($SPIB^-$) and M ($GP2^+$) cells. Cell's morphology is identified by staining of F-actin using Phalloidin (red/white). Three independent experiments are performed on one donor with similar results. Scale bars, 10 µm. (**i,j**) Representative confocal images (**i**) and numbers of bacteria particles (**j**) in 2D-cultured M cells treated w/wo Cytochalasin B (CytoB). Bacteria particles are labeled in red. n = 10 cells examined over 2 independent experiments on one donor. Each dot represents one cell. Data are presented as mean values +/− SEM. P-values are derived from two-tailed t-test. Scale bars, 10 µm. (**k**) Violin plots showing the expression levels of MHC-II genes and *CD74* between M cells and enterocytes in M cell organoid-derived scRNA-seq dataset containing 375 cells. (**l**) Representative flow cytometry analysis of MHC-II and ICAM2 expression in cultured M cell organoids derived from two donors. For each donor, three independent experiments are performed with similar results. (**m**) qPCR analysis of the expression levels of a set of M cell markers in sorted $MHC\text{-}II^-$ and $MHC\text{-}II^+$ cells. Two donors are shown. For each donor, n = 3 technical replicates are shown. Data are presented as mean values +/− SEM. P-values are derived from two-tailed t-test. (**n**) Validation of *CIITA* KO by targeted genotyping.

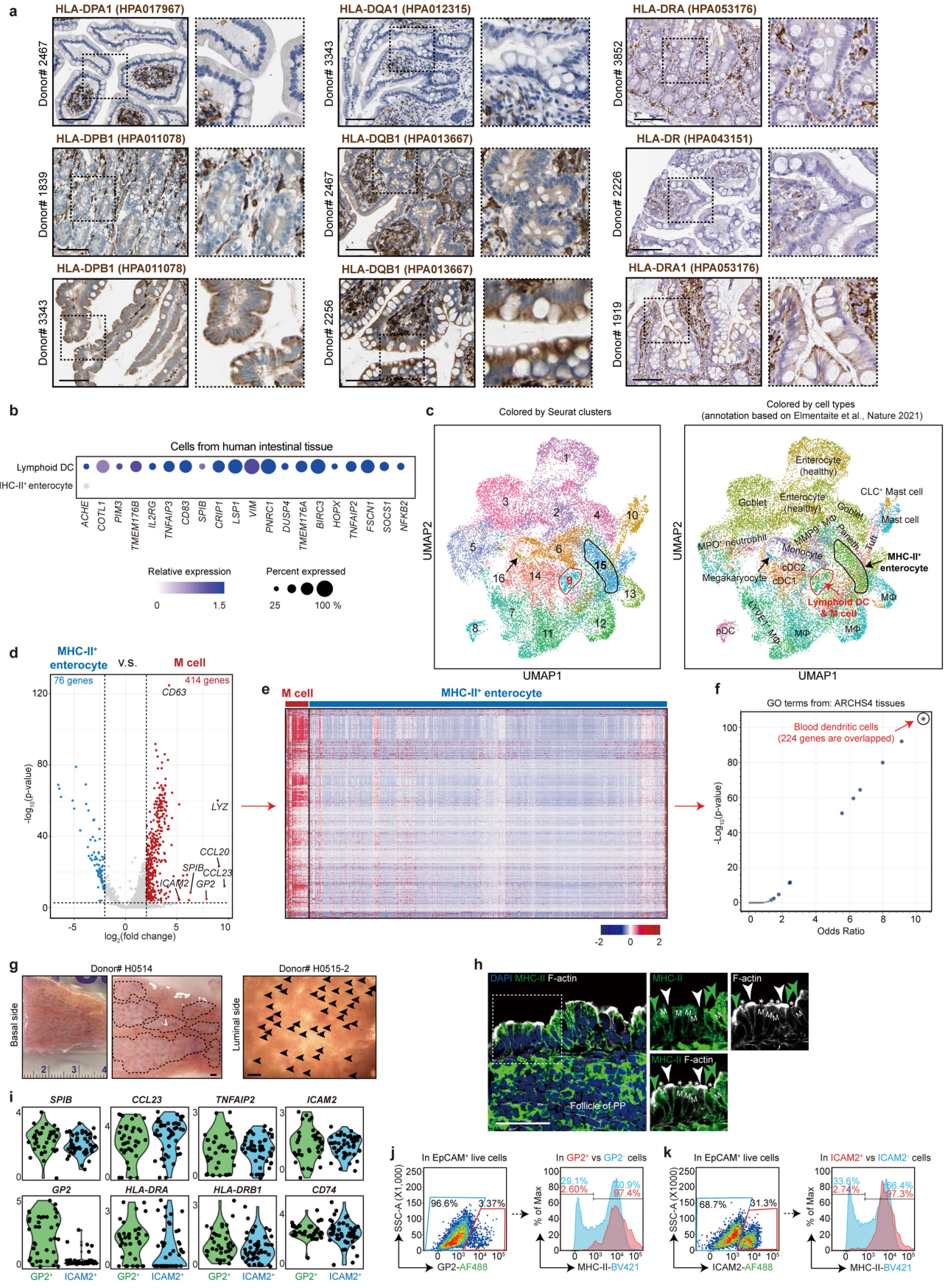

Extended Data Fig. 6 | See next page for caption.

Extended Data Fig. 6 | Analysis of MHC-II expression in human M cells and enterocytes. (**a**) IHC staining with antibodies directed against MHC-II proteins (HLA-DP/DQ/DR) on the human intestinal tissue sections. Positive staining signals of MHC-II can be detected in immune cells across all samples and in the enterocytes of several samples (the bottom panels). Images are derived from the Human Protein Atlas (proteinatlas.org). Similar results are observed on tissues from 5 donors (upper and middle panels) and 3 donors (bottom panels). Scale bars, 50 μm. (**b**) Dot plot showing the expression levels of a set of lymphoid DC markers in primary lymphoid DCs versus MHC-II$^+$ enterocytes. n = 2,665 single cells. Dot color relates to normalized mean expression values and dot size to fraction of expressing cells. (**c**) scRNA-seq analysis of primary human intestinal cells. Multiple epithelial and immune cell types are integrated unbiasedly. n = 22,672 single cells. Cell clusters are visualized in UMAP plots and colored by unsupervised clustering (left) or annotated cell types (right). M cells and lymphoid DCs are clustered together (in cluster #9, as indicated by the red circles). MHC-II$^+$ enterocytes (cluster #15, as indicated by the black circles) are not clustered with DC subtypes. (**d,e**) Volcano plot (**d**) and heatmap (**e**) showing the DEGs between primary M cells and MHC-II$^+$ enterocytes. P-values are derived from two-sided Wald test in (**d**). (**f**) Volcano plot showing the GO analysis based on the up-regulated DEGs in primary M cells, identifying the most relevant cell type to be DCs, with 224 DEGs overlapping with DC genes. P-values are derived from one-sided Fisher's exact test. (**g**) Representative images showing the PPs enriched in human terminal ileum tissues. The basal and luminal sides of the tissue are shown on two donors, respectively. Scale bar, 1 mm in the right panel. (**h**) Representative confocal images showing the MHC-II$^+$ cells in human PP epithelium. MHC-II$^+$ cells are identified by MHC-II antibody staining (green, detected in both cytoplasm and primarily on basolateral surface of the cells). Microvilli structures are detected by staining of F-actin using Phalloidin (white). MHC-II$^+$ M cell with fewer microvilli (mature M cell) are marked by asterisks. MHC-II$^+$ and MHC-II$^-$ FAE cells with normal microvilli are indicated by green and white arrows, respectively. M, mature M cell. Similar results are observed on PP tissues from two donors. Scale bar, 50 μm. (**i**) Violin plots showing the expression levels of M cell markers, MHC-II genes and CD74 in primary ICAM2$^+$GP2$^-$ and GP2$^+$ M cells. n = 88 single cells. Each dot represents a single cell. (**j,k**) Representative flow cytometry analysis of MHC-II expression in GP2$^+$ (**j**) or ICAM2$^+$ (**k**) primary M cells. Similar results are observed in PP tissues from two unrelated donors.

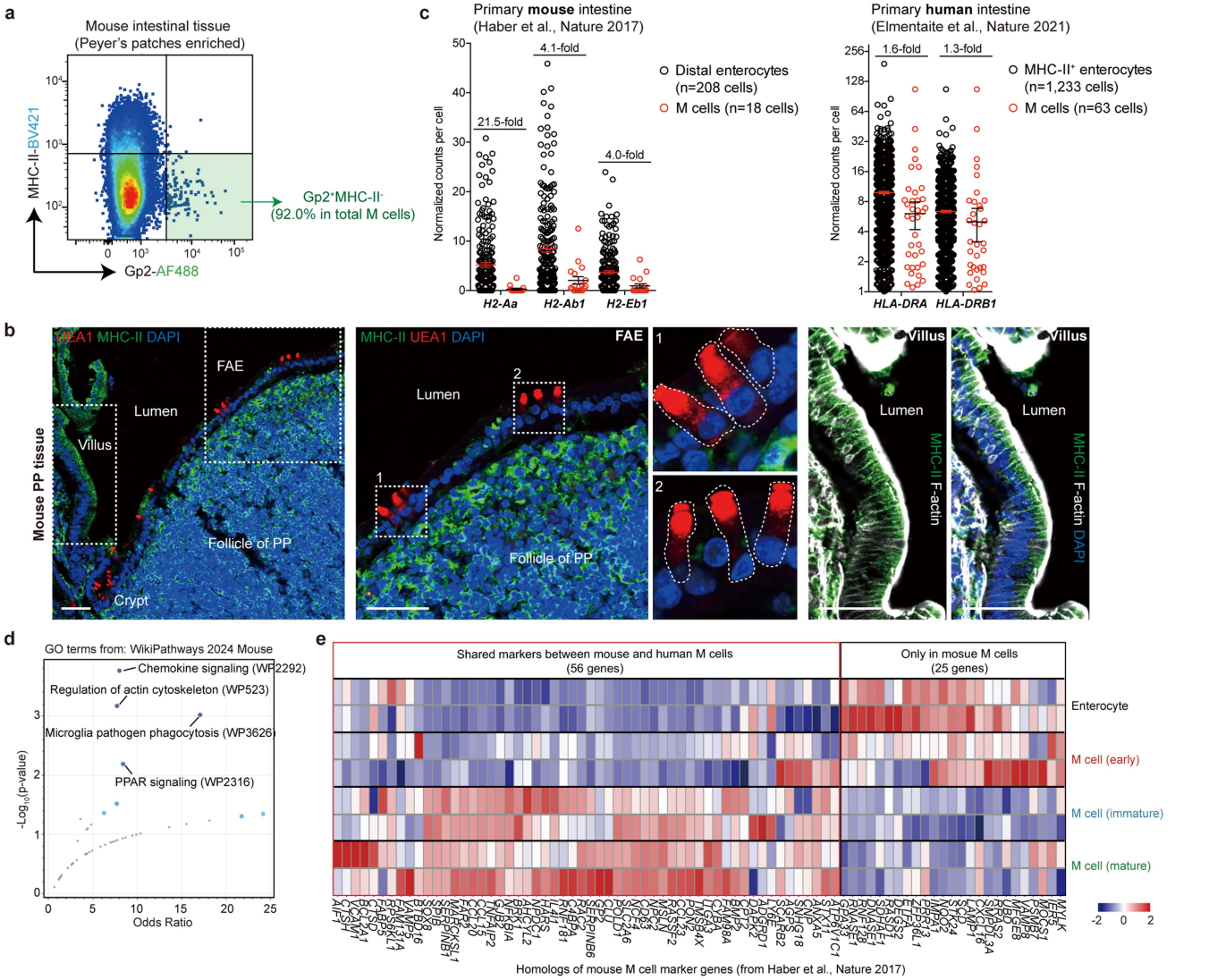

Extended Data Fig. 7 | Analysis of MHC-II expression in murine M cells and enterocytes. (**a**) Representative flow cytometry analysis of MHC-II and Gp2 expression in primary mouse intestinal tissues. Results are representative of three independent experiments. A total of 59 PPs from n = 10 mice are enriched through microdissection. (**b**) Representative confocal images showing the MHC-II$^+$ cells in mouse villus epithelium and FAE. MHC-II$^+$ cells are identified by MHC-II antibody staining (green, detected in both cytoplasm and on cell surface of the villus epithelium). Cells are outlined by staining of F-actin using Phalloidin (white). M cells are marked by UEA-1 staining (in red) and show negative staining for MHC-II. Three independent experiments on PPs derived from n = 10 mice are performed with similar results. Scale bars, 50 µm. (**c**) Normalized counts of MHC-II genes in MHC-II$^+$ enterocytes and M cells. Data are derived from scRNA-seq datasets of primary mouse and human intestinal cells, respectively. Data are presented as mean values +/− SEM. Each dot represents a single cell. (**d**) volcano plot showing the GO analysis based on the murine M cell markers (97 genes from primary and organoid M cells), identifying pathways related to the conventional M cell functions. P-values are derived from one-sided Fisher's exact test. (**e**) Heatmap showing the gene expression levels of murine M cell marker genes (81 human homologs out of the 97 murine M cell markers) across the indicated cell populations in human M cell organoid dataset. n = 2 biological replicates.

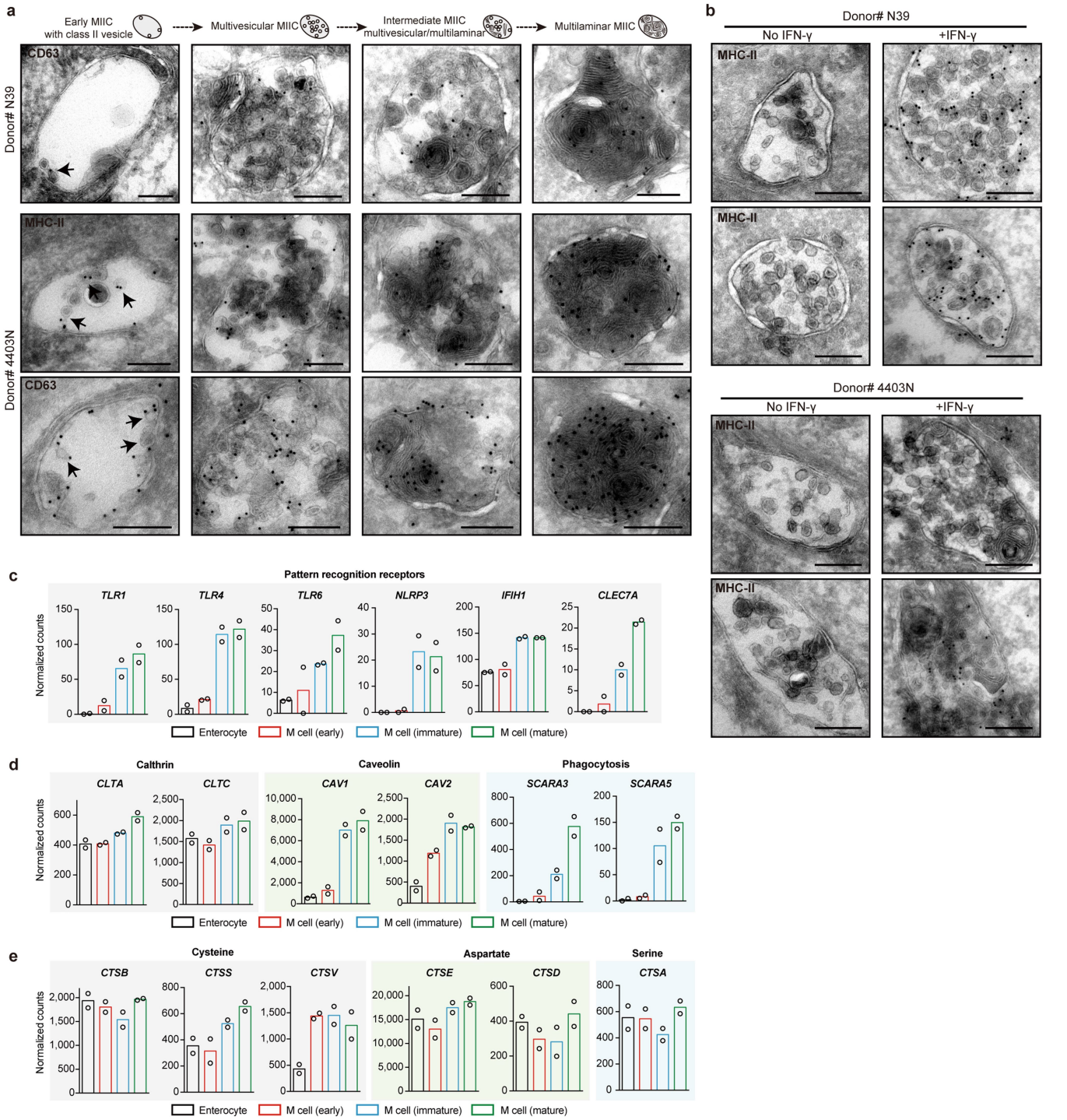

Extended Data Fig. 8 | Human M cells contain MIIC structures for antigen processing and loading, and express genes that are related to pathogen recognition, antigen uptake and protein digestion. (**a**) Representative immuno-electron microscopy images showing MIIC structures in endosomes, identified by immunogold staining of MHC-II or CD63 antibody, in organoid M cells. Arrows indicate the MHC-II vesicles in the endosome. M cell organoids from two donors are tested with similar results. Scale bars, 200 nm. (**b**) Representative immuno-electron microscopy images showing the endosomes with MHC-II vesicles, identified by immunogold staining of MHC-II antibody, in normal intestinal organoids treated with IFN-γ. Organoids from two donors are tested with similar results. Scale bars, 200 nm. (**c-e**) Expression levels (normalized counts) of pattern recognition receptors (**c**), antigen uptake (**d**) and protein digestion (**e**) related genes across the indicated cell populations. n = 2 biological replicates. Data are presented as mean values.

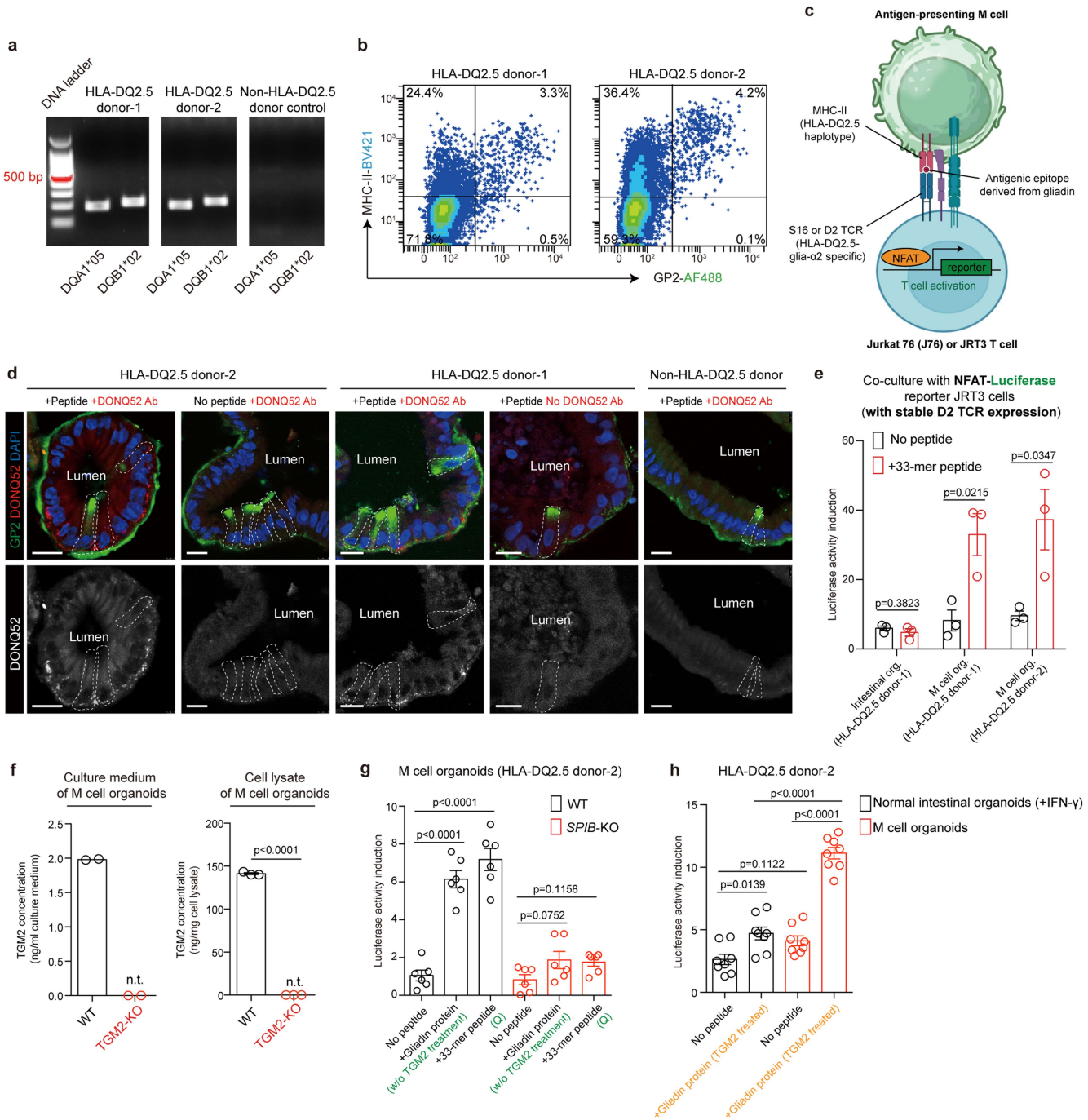

Extended Data Fig. 9 | Gluten antigen presentation in human M cell organoids. (**a**) Representative genotyping PCR for HLA-DQ2.5 haplotype. Two independent experiments are performed with similar results. For gel source data, see Supplementary Fig. 1. (**b**) Representative flow cytometry analysis of MHC-II and GP2 expression in M cell organoids derived from two HLA-DQ2.5 donors. For each donor, three independent experiments are performed with similar results. (**c**) Schematic model of antigen presentation in CeD using human M cell organoids. Images were created in BioRender. van Es, J. (2025) https://BioRender.com/xh7haut. (**d**) Representative confocal images of DONQ52 antibody staining in M cell organoids derived from multiple donors. 33-mer peptide is added to the organoids before staining. M cells are marked by IF staining of GP2 antibody (green). DONQ52 antibody specifically recognizes the gliadin peptide:HLA-DQ2.5 complexes (red/white). In each condition, three independent experiments are performed on two donors with similar results. Scale bars, 20 µm. (**e**) Quantification of luciferase activity in reporter T cells after co-culture with organoids treated w/wo 33-mer peptide. Two HLA-DQ2.5 donors are tested. For each donor, n = 3 biological replicates. Each dot represents one biological replicate. Data are presented as mean values +/− SEM. P-values are derived from two-tailed t-test. (**f**) Quantification of TGM2 protein levels in M cell organoids (WT versus *TGM2*-KO) and their culture media by ELISA. n = 2 or 3 independent wells on one donor. Each dot represents one well. Data are presented as mean values or mean values +/− SEM. P-values are derived from two-tailed t-test. n.t. not detected. (**g**) Quantification of luciferase activity in reporter T cells after co-culture with WT or *SPIB*-KO M cell organoids treated w/wo indicated peptides. n = 6 biological replicates on one donor. Each dot represents one biological replicate. Data are presented as mean values +/− SEM. P-values are derived from one-way ANOVA with Dunnett's test. (**h**) Quantification of luciferase activity in reporter T cells after co-culture with organoids treated w/wo gliadin proteins. n = 8 biological replicates on one donor. Each dot represents one biological replicate. Data are presented as mean values +/− SEM. P-values are derived from one-way ANOVA with Tukey's test.

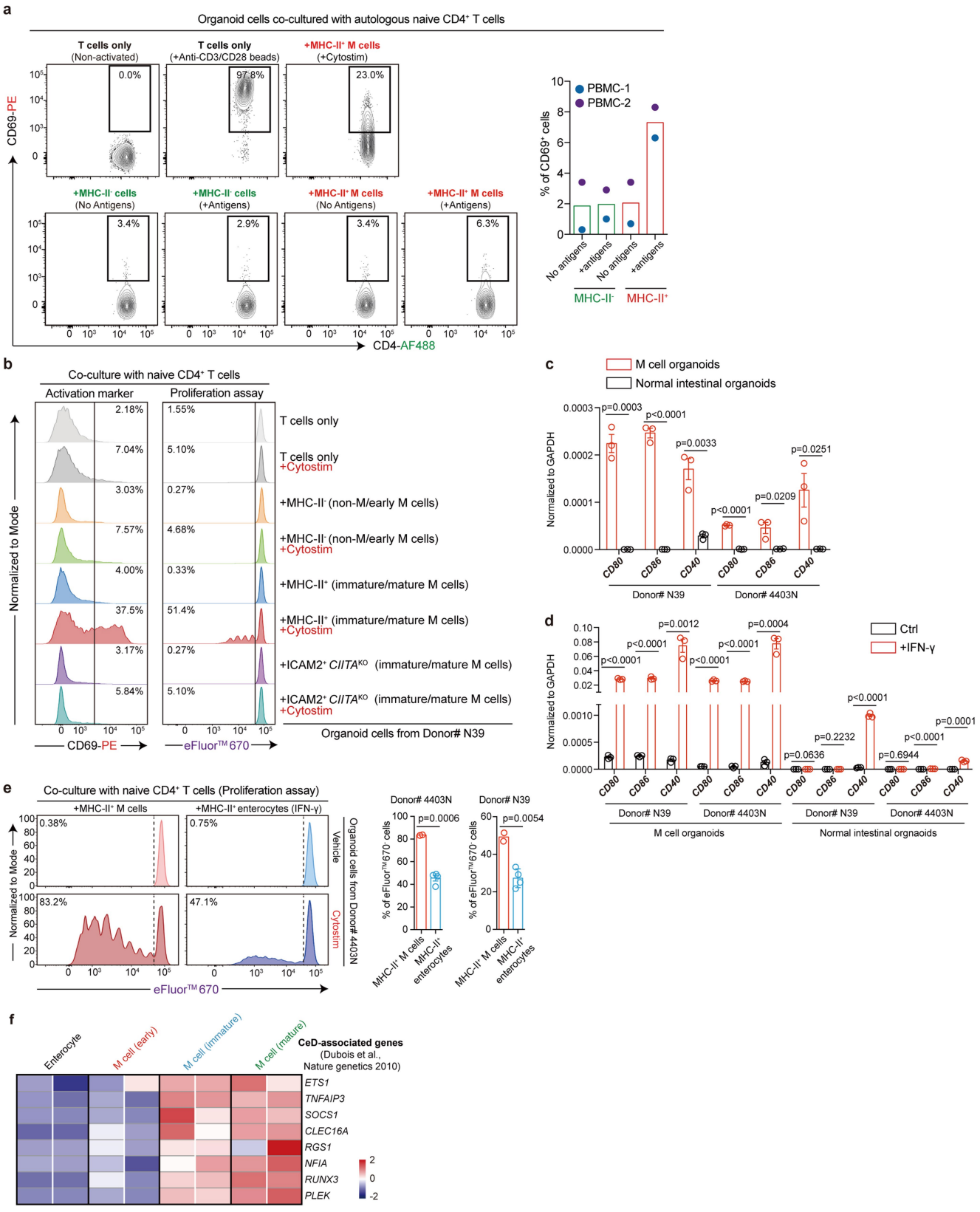

Extended Data Fig. 10 | See next page for caption.

Extended Data Fig. 10 | Naïve T cell activation by M cell-mediated antigen presentation. (**a**) Activation of autologous naïve $CD4^+$ T cells, quantified by flow cytometry analysis of $CD69^+$ cell percentage, after co-culture with MHC-$II^{+/-}$ cells treated w/wo the antigen cocktail. $CD69^+$ cells are gated based on the negative control group in which T cells are not activated (w/o treatment). Activated T cells by anti-CD3/CD28 beads are used as positive control. Autologous naïve T cells are isolated from PBMCs. Two unrelated donors are analyzed. Each dot represents the mean value derived from two independent wells. Data are presented as mean values of the two donors. (**b**) Flow cytometry analysis of primary naïve $CD4^+$ T cell activation and proliferation after co-culture with MHC-$II^{+/-}$ cells treated w/wo Cytostim. MHC-$II^{+/-}$ cells are FACS-sorted from M cell organoids derived from two donors. Similar results are observed on the two donors. Representative results from one donor is shown. Each group is analyzed based on two independent co-culture wells with similar results. In *CIITA*-KO M cell organoids, immature and mature M cells do not express MHC-II. Thus, M cells are sorted based on ICAM2 antibody staining instead of MHC-II. (**c**) qPCR analysis of the expression levels of co-stimulatory molecules (*CD80*, *CD86*, and *CD40*) in M cell organoids versus normal intestinal organoids. Two donors are shown. For each donor, n = 3 technical replicates are shown. Data are presented as mean values +/− SEM. P-values are derived from two-tailed t-test. Results are representative of two independent experiments. (**d**) qPCR analysis of the expression levels of co-stimulatory molecules (*CD80*, *CD86*, and *CD40*) in M cell organoids versus normal intestinal organoids. Organoids are treated w/wo IFN-γ. Two donors are shown. For each donor, n = 3 technical replicates are shown. Data are presented as mean values +/− SEM. P-values are derived from two-tailed t-test. Results are representative of two independent experiments. (**e**) Flow cytometry analysis of primary naïve $CD4^+$ T cell proliferation after co-culture with MHC-II^+ M cells or MHC-II^+ enterocytes treated w/wo Cytostim. MHC-II^+ cells are FACS-sorted from M cell organoids or IFN-γ treated intestinal organoids, respectively. Organoids derived from two donors are shown. For each donor, n = 2 and 4 independent co-culture wells for M cell and enterocytes, respectively. Data are presented as mean values or mean values +/− SEM. P-values are derived from two-tailed t-test. (**f**) Heatmap showing the expression patterns of a set of CeD-associated genes during M cell differentiation. n = 2 biological replicates.

nature portfolio

Corresponding author(s): Hans Clevers

Last updated by author(s): Sep 15, 2025

Reporting Summary

Nature Portfolio wishes to improve the reproducibility of the work that we publish. This form provides structure for consistency and transparency in reporting. For further information on Nature Portfolio policies, see our Editorial Policies and the Editorial Policy Checklist.

Statistics

For all statistical analyses, confirm that the following items are present in the figure legend, table legend, main text, or Methods section.

n/a	Confirmed	
☐	☒	The exact sample size (*n*) for each experimental group/condition, given as a discrete number and unit of measurement
☐	☒	A statement on whether measurements were taken from distinct samples or whether the same sample was measured repeatedly
☐	☒	The statistical test(s) used AND whether they are one- or two-sided *Only common tests should be described solely by name; describe more complex techniques in the Methods section.*
☒	☐	A description of all covariates tested
☐	☒	A description of any assumptions or corrections, such as tests of normality and adjustment for multiple comparisons
☐	☒	A full description of the statistical parameters including central tendency (e.g. means) or other basic estimates (e.g. regression coefficient) AND variation (e.g. standard deviation) or associated estimates of uncertainty (e.g. confidence intervals)
☐	☒	For null hypothesis testing, the test statistic (e.g. *F*, *t*, *r*) with confidence intervals, effect sizes, degrees of freedom and *P* value noted *Give P values as exact values whenever suitable.*
☒	☐	For Bayesian analysis, information on the choice of priors and Markov chain Monte Carlo settings
☒	☐	For hierarchical and complex designs, identification of the appropriate level for tests and full reporting of outcomes
☒	☐	Estimates of effect sizes (e.g. Cohen's *d*, Pearson's *r*), indicating how they were calculated

Our web collection on statistics for biologists contains articles on many of the points above.

Software and code

Policy information about availability of computer code

Data collection	BD FACS Influx, BD LSR Fortessa X20, BD FACSMelody, Leica SP8 confocal detection system fitted on a Leica DMi8 microscope, Bio-Rad CFX Connect Real-Time PCR machine, Tecnai T12 electron microscope equipped with an Eagle 4kX4k CCD camera, TECAN Spark® multimode microplate reader.
Data analysis	R studio (v3.6.3), Python (v3.11.9), Seurat R package (v3.1.4), DEseq2 R package (1.26.0), clusterProfiler R package (v3.14.3), Enrichr web software (http://maayanlab.cloud/Enrichr), GraphPad PRISM (v7.04), FlowJo (v10.8.0), BD FACS Diva software (v8.0.1), Leica LAS X software (v3.5.7.23225), IMARIS software (v9.3).

For manuscripts utilizing custom algorithms or software that are central to the research but not yet described in published literature, software must be made available to editors and reviewers. We strongly encourage code deposition in a community repository (e.g. GitHub). See the Nature Portfolio guidelines for submitting code & software for further information.

Data

Policy information about availability of data

All manuscripts must include a data availability statement. This statement should provide the following information, where applicable:

- Accession codes, unique identifiers, or web links for publicly available datasets
- A description of any restrictions on data availability
- For clinical datasets or third party data, please ensure that the statement adheres to our policy

The organoid scRNA-seq and bulk RNA-seq datasets generated in this study have been deposited and are publicly available in the Gene Expression Omnibus (GEO, www.ncbi.nlm.nih.gov/geo/) under accession codes GSE275771 and GSE275772. We re-analyzed the following publicly available scRNA-seq datasets: GSE119969 (GSM3389578, GSM3389579 and GSM3389580; URL: www.ncbi.nlm.nih.gov/geo/query/acc.cgi?acc=GSE119969), GSE125970 (raw_UMIcounts.txt.gz; URL: www.ncbi.nlm.nih.gov/geo/query/acc.cgi?acc=GSE125970), GSE146799 (EEC_atlas_raw.csv.gz; URL: www.ncbi.nlm.nih.gov/geo/query/acc.cgi?acc=GSE146799), GSE92332 (FAE_UMIcounts.txt.gz and Org_RANKL_UMIcounts.txt.gz; URL: www.ncbi.nlm.nih.gov/geo/query/acc.cgi?acc=GSE92332), and Space-Time Gut Cell Atlas (datasets for epithelium and myeloid cells; URL: www.gutcellatlas.org).

Research involving human participants, their data, or biological material

Policy information about studies with human participants or human data. See also policy information about sex, gender (identity/presentation), and sexual orientation and race, ethnicity and racism.

Reporting on sex and gender	Both male and female were included.
Reporting on race, ethnicity, or other socially relevant groupings	N/A
Population characteristics	No data on population characteristics was collected/used.
Recruitment	Ileum and colon tissues were obtained from adult patients undergoing tumor–resection surgery. Tissues were collected at an appropriate distance from the tumor.
Ethics oversight	Two terminal ileum tissues (Donor# H0514 and H0515-2) for IF staining and flow cytometry analysis were obtained from Diakonessen Hospital Utrecht, with approval by the Medical Ethical Committee of the hospital and with informed consent of each patient. The CeD patient PBMCs were collected from participants of the CeDNN study. CeDNN was approved by the Medical Ethical Committee of the University Medical Center Groningen, with the METc No. 2013/440. Written consent was signed by all participants, their parents, or legal representatives for participants aged under 16 for CeDNN. Normal PBMCs were purchased from Sanquin (Amsterdam), with signed Material Transfer Agreement (MTA). A total of five human intestinal organoid lines were established in our lab and recruited in this study. Three ileum tissues (Donor# 12339, 4280N/HLA-DQ2.5 #1, 4403N/HLA-DQ2.5 #2) were obtained from the Netherlands Cancer Institute (NKI); One ileum tissue (Donor# N39) and one colon tissue (Donor# P11N) were obtained from the Diakonessen Hospital Utrecht, all with approval by the Medical Ethical Committee of the respective organizations and with informed consent of each patient. This study was approved by the Ethical Committee of Hubrecht Institute and was in accordance with the Declaration of Helsinki and according to the Dutch law. The study complied with all relevant guidelines and regulations regarding research involving human participants.

Note that full information on the approval of the study protocol must also be provided in the manuscript.

Field-specific reporting

Please select the one below that is the best fit for your research. If you are not sure, read the appropriate sections before making your selection.

☒ Life sciences ☐ Behavioural & social sciences ☐ Ecological, evolutionary & environmental sciences

For a reference copy of the document with all sections, see nature.com/documents/nr-reporting-summary-flat.pdf

Life sciences study design

All studies must disclose on these points even when the disclosure is negative.

Sample size	No sample size calculation was performed. Unlike in mouse study, organoid experiments were all conducted in a highly controlled environment, and only involve specific cells or molecules rather than whole organism. For quantitative organoid experiments, based on our experience, experimental triplicates is sufficient for comparisons between groups and

	answering our scientific questions (i.e., PMID: 36002022). Twenty randomly selected organoids per experimental group are also sufficient. (i.e., PMID: 40010349). For organoid experiments that do not require quantification, based on our experience, the variables in these experiments are limited, results are highly significant and consistent based on 2 or 3 biological replicates (i.e., PMID: 39418382).
Data exclusions	No data points were excluded.
Replication	All experiments were performed in multiple biological replicates and in several organoid lines derived from unrelated donors. Detailed information was indicated in the text and figure legends.
Randomization	Organoids from the same batch/passage but cultured in different wells were randomized into different experimental groups before the different treatments. After treatment, for the analysis that are not based on single organoids (i.e., FACS, qPCR), all the organoids in each well were collected, thus no randomization is required. For the analysis on single organoids, the organoids in each experimental group were randomly selected and quantified. For experiments that do not involve a statistic comparisons (i.e., confirmation of marker gene expression by IF staining) but just phenotype observations, randomization is considered not relevant.
Blinding	The researchers were not blinded since all of our experiments are nonclinical studies which has been conducted in a laboratory setting, and outcomes are all coming from objective measurements, we considered blinding is not relevant for our study.

Reporting for specific materials, systems and methods

We require information from authors about some types of materials, experimental systems and methods used in many studies. Here, indicate whether each material, system or method listed is relevant to your study. If you are not sure if a list item applies to your research, read the appropriate section before selecting a response.

Materials & experimental systems

n/a	Involved in the study
☐	☒ Antibodies
☐	☒ Eukaryotic cell lines
☒	☐ Palaeontology and archaeology
☐	☒ Animals and other organisms
☒	☐ Clinical data
☒	☐ Dual use research of concern
☒	☐ Plants

Methods

n/a	Involved in the study
☒	☐ ChIP-seq
☐	☒ Flow cytometry
☒	☐ MRI-based neuroimaging

Antibodies

Antibodies used	Antibodies for immuno staining: mouse anti-human GP2 antibody (MBL, Cat# D277-3, clone# 3G7-H9, diluted in 1:200); mouse anti-human ICAM2 antibody (Thermo Fisher, Cat# BMS109BT, clone# CBR-IC2/2, diluted in 1:200); mouse anti-human HLA-DP/DQ/DR antibody (Thermo Fisher, Cat# MA1-25914, clone# CR3/43, diluted in 1:200); Phalloidin (Sigma, Cat# 65906-10NMOL, diluted in 1:1000); DONQ52 antibody (kindly provided by Chugai Pharmaceutical Co. Ltd., Tokyo, Japan, diluted in 1:100); Rat anti-mouse MHC-II (I-A/I-E) antibody (Thermo Fisher, Cat# 14-5321-82, clone# M5/114.15.2, diluted in 1:200); UEA-1-Rhodamine (Vector, Cat# RL-1062-2, diluted in 1:1000). Antibodies for flow cytometry (all diluted in 1:100): mouse anti-human GP2-AF488 antibody (MBL, Cat# D277-A48, clone# 3G7-H9); rat anti-mouse Gp2-AF488 antibody (MBL, Cat# D278-A48, clone# 2F11-C3); mouse anti-human ICAM2-biotin antibody (Thermo Fisher, Cat# BMS109BT, clone# CBR-IC2/2); mouse anti-human HLA-DP/DQ/DR-BV421 antibody (BD horizon, Cat# 564244, clone# Tu39); mouse anti-human TCR-APC antibody (Biolegend, Cat# 3-6718, clone# IP26). mouse anti-human HLA-DP/DQ/DR-FITC antibody (BD Pharmingen, Cat# 562008, clone# Tu39); mouse anti-human CD4-AF488 antibody (Biolegend, Cat# 317420, clone# OKT4); mouse anti-human EpCAM-APC antibody (Biolegend, Cat# 369810, clone# CO17-1A); mouse anti-human CD69-PE antibody (Biolegend, Cat# 310905, clone# FN50); Rat anti-mouse MHC-II (I-A/I-E)-BV421 antibody (Biolegend, Cat# 107631, clone# M5/114.15.2); Rat anti-mouse CD45-PE (Biolegend, Cat# 103106, clone# 30-F11); Rat anti-mouse EpCAM-APC (Thermo Fisher, Cat# 17-5791-80, clone# G8.8). Antibodies for immuno electron microscopy (all diluted in 1:20): Mouse anti-human CD63 antibody (BD Biosciences, Cat# 556019, clone# H5C6); mouse anti-human HLA-DP/DQ/DR antibody (Thermo Fisher, Cat# MA1-25914, clone# CR3/43).
Validation	All the antibodies are widely used and validated in the field. Listed examples: Anti-GP2/Gp2 antibodies were validated in previous studies: PMID: 32247021 and PMID: 19907495. Anti-ICAM2 antibody was validated in previous studies: PMID: 34484188 and PMID: 21191062.

HLA-DP/DQ/DQ antibodies were validated in previous studies: clone# CR3/43 PMID: 31348891; clone# Tu39 PMID: 18039949.
DONQ52 antibody was validated in previous study: PMID: 38135691.
MHC-II (I-A/I-E) antibodies were validated in previous studies: PMID: 19047439 and PMID: 16973389.
Anti-TCR antibody was validated in previous study: PMID:31150624.
CD4 antibody was validated in previous study: PMID: 35551746.
EpCAM antibodies was validated in previous studies: clone# CO17-1A PMID: 33096021; clone# G8.8 PMID: 37587341.
CD69 antibody was validated in previous study: PMID: 34099545.
CD45 antibody was validated in previous studies: PMID: 16709810.
CD63 antibody was validated in previous study: PMID: 32049054.

Eukaryotic cell lines

Policy information about cell lines and Sex and Gender in Research

Cell line source(s)	Human intestine tissues were obtained from the Netherlands Cancer Institute (NKI) and Diakonessen Hospital Utrecht. All the human adult intestine organoid lines were derived from non-transformed, normal mucosa of the patients. Resection specimen was obtained as residual material after clinical procedures in accordance with the Declaration of Helsinki and the ethical guidelines of the respective organizations. Donor# P11N, human colon organoid line; Female. Donor# 12339, human ileum organoid line; Male. Donor# N39, human ileum organoid line; Female. Donor# 4280N, human ileum organoid line. Donor# 4403N, human ileum organoid line. The human Jurkat T cell line derivative JRT3 cell line, with endogenous TCRα and TCRβ chains knockout, expressing NFAT-RE-Luc2 and HLA-DQ2.5-glia-α2 specific TCR D2, was kindly provided by Chugai Pharmaceutical Co. Ltd. (Tokyo, Japan). The human Jurkat T cell line derivative J76 reporter cell line (J76TPR), was kindly provided by Dr. Mirjam H.M. Heemskerk.
Authentication	None of the organoid lines used were authenticated. For the two reporter Jurkat T cell lines expressing gliadin-specific TCRs and reporter genes, both cell lines were validated based on gliadin-specific T cell activation, as indicated by the induced reporter gene expression.
Mycoplasma contamination	All organoid lines and cell lines were assessed and scored negative for mycoplasma contamination.
Commonly misidentified lines (See ICLAC register)	No commonly misidentified cell lines were used.

Animals and other research organisms

Policy information about studies involving animals; ARRIVE guidelines recommended for reporting animal research, and Sex and Gender in Research

Laboratory animals	Wild-type (WT) C57BL/6 mice were involved in this study.
Wild animals	The study did not involve wild animals.
Reporting on sex	Both male (n=2) and female (n=8) adult mice (>8 wks) were collected and included in this study.
Field-collected samples	The study did not involve samples collected from the field, mice were housed in the standard SPF unit.
Ethics oversight	No specific ethical guidance was required, as in this study, we only collected the intestinal Peyer's patches from sacrificed WT B6 mice, which is approved by the Institutional Review Board of Hubrecht Institute.

Note that full information on the approval of the study protocol must also be provided in the manuscript.

Plants

Seed stocks	N/A
Novel plant genotypes	N/A
Authentication	N/A

Flow Cytometry

Plots

Confirm that:

☒ The axis labels state the marker and fluorochrome used (e.g. CD4-FITC).

☒ The axis scales are clearly visible. Include numbers along axes only for bottom left plot of group (a 'group' is an analysis of identical markers).

☒ All plots are contour plots with outliers or pseudocolor plots.

☒ A numerical value for number of cells or percentage (with statistics) is provided.

Methodology

Sample preparation	Organoids were released from BME using ice-cold Corning Cell Recovery Solution (Sigma-Aldrich, Cat# CLS354253) and were dissociated with 1 ml TripLE at 37 °C for 6-8 mins, followed by gently pipetting 20 times. After TripLE dissociation, the cell suspension was filtered through a 40 µm cell strainer and stained with DAPI or PI for flow cytometry analysis or FACS sorting. The human terminal ileum tissue was first dissected to remove the muscularis externa, following a previous protocol. Regions containing human or mouse Peyer's patches, which could be clearly identified under dissection microscopy, were enriched, minced into small pieces (~1 mm^2), and digested in digestion buffer (adDMEM/F12 supplemented with 100 U/ml P/S, 10 mM HEPES, 1× GlutaMAX, 1 mg/ml collagenase (Sigma-Aldrich, Cat# C9407), and 5 mM EDTA) for 30 minutes at 37°C, with vigorous shaking every 5 minutes. The digested tissues were then filtered through a 100 µm cell strainer, washed twice with wash buffer (adDMEM/F12 supplemented with 100 U/ml P/S, 10 mM HEPES, 1× GlutaMAX, and 10% FBS), and dissociated into single cells for flow cytometry analysis, similar to the procedure used for organoids, as described above.
Instrument	Samples were analyzed on a BD LSR Fortessa X20 equipped with 4 lasers (BD Bioscience) or BD FACSMelody equipped with 3 lasers (BD Bioscience). Cell sorting was performed on a BD FACS Influx cell sorter equipped with 5 lasers (BD Bioscience).
Software	FACS Diva (v8.0.1), FlowJo (v10.8.0).
Cell population abundance	Purity of the sorted cells were validated by qPCR analysis or RNA-sequencing as shown in Fig. 1g, Fig. 2g, Fig. 3d, ED Fig. 1i, ED Fig. 2b, ED Fig. 5b and ED Fig. 5m.
Gating strategy	Cells were identified based on FSC and SSC gating. Live single cells were identified as is shown in the gating strategies included in Supplementary Figure 2. Briefly: Gate1: SSC-A/FSC-A to identify the cell fraction. Gate2: FSC-H/FSC-W to remove doublets in intestinal epithelial cells. FSC-H/FSC-A to remove doublets in T cells. Gate3: DAPI or PI staining to select the negative population as live cells. Gate4: EpCAM staining to select epithelial cells from intestinal tissue. CD4 or TCR staining to select T cells of interest. Gate5: Analysis of the reporter fluorophores and antibody staining signals as shown in the figures. Boundaries were defined based on comparison with the negative control cells without any fluorophore. Full sequential gating strategies are included in Supplementary Figure 2.

☒ Tick this box to confirm that a figure exemplifying the gating strategy is provided in the Supplementary Information.